NKS-326
ISBN 978-87-7893-407-9

Effects of dynamic behaviour of Nordic marine environment to radioecological assessments

Halldórsson[1] Ó.
Iosjpe[2] M.
Isaksson[3] M.
Joensen[4] H. P.
Jonsson[1] G.
Logemann[5] K.
Roos[6] P.
Suolanen[7] V.
Thomas[3] R.
Vartti[8] V.-P.

1 Icelandic Radiation Safety Authority
2 Norwegian Radiation Protection Authority
3 University of Gothenburg, Sweden
4 University of the Faroe Islands
5 University of Iceland
6 Technical University of Denmark
7 Technical Research Centre of Finland
8 Radiation and Nuclear Safety Authority, Finland

January 2015

Abstract

The goal of the EFMARE project is an analysis of consequences of radioactive releases into marine environment with special attention to the effects of the dynamic behaviour of the Nordic seas to radioecological assessments. The EFMARE project activity has planned to continue for two years (2014-2015).
The main goals for 2014 is development and implementation of the bioaccumulation process into the models, improvement of the models, comparison with previous results and testing of the influence of the time of an accident for the radioecological consequences.
Results of implementation of the kinetic model for bioaccumulation processes into the NRPA box model and the DETRA computer code clearly demonstrated that there is a significant quantitative difference between the kinetic modelling approach and the approach based on the constant concentration rates.
Results of modelling were compared with experimental data on the basis of improved version of the NRPA box model for the Baltic Sea. It is clear demonstration that dynamic modelling of the bioaccumulation processes can provide a more correct description of the concentration of radionuclides in biota and, therefore, these results support the main goal of the EFMARE project.
With a numerical case study the temporal variability of pollutant dispersal in Icelandic waters was demonstrated and discussed. The results emphasize the necessity to use operational hydrodynamic ocean models in order to forecast pollutant dispersal in Icelandic waters.
The use of particle density can be used for comparison with simulations from the NRPA box model.

Key words

marine environment, hydrodynamic and box modelling, bioaccumulation submodel, accidents, radioecological consequences

NKS-326
ISBN 978-87-7893-407-9

Electronic report, January 2015
NKS Secretariat
P.O. Box 49
DK - 4000 Roskilde, Denmark
Phone +45 4677 4041
www.nks.org
e-mail nks@nks.org

Effects of dynamic behaviour of Nordic marine environment to radioecological assessments (EFMARE)

Interim Report for the NKS-B EFMARE activity 2014
Contract AFT/B(14)12

Contributors:

Halldórsson Óskar, Geislavarnir Rikisins, Iceland
Iosjpe Mikhail, Norwegian Radiation Protection Authority, Norway
Isaksson Mats, University of Gothenburg, Sweden
Joensen Hans Pauli, Fróðskaparsetur Føroya, Faroe Islands
Jonsson Gisli, Geislavarnir Rikisins, Iceland
Logemann Kai, University of Iceland, Iceland
Roos Per, Technical University of Denmark, Denmark
Suolanen Vesa, Technical Research Centre of Finland, Finland
Thomas Rimon, University of Gothenburg, Sweden
Vartti Vesa-Pekka, Radiation and Nuclear Safety Authority, Finland

December 2014

Content

1. Introduction

According to the proposed activity under the course of the EFMARE project, analysis of consequences of severe radioactive releases to Nordic marine environment will be provided with special attention to the effects of the dynamic behaviour of the Nordic marine environment to radioecological assessments.

The analysis of the consequences of some hypothetical NPP and submarine reactor accidents in the coastal Nordic marine environment (Loviisa, Olkiluoto, Finland; Forsmark, Sweden; Icelandic and Faroese coastal areas; Belt Sea, Denmark) indicates a clear possibility for improvement of the present evaluation by a more detailed modelling of the key processes for radioecological assessment and by evaluating the environmental sensitivity of the Nordic marine environment.

High concentrations of radionuclides in fish, detected long time after the Fukushima accident, have also supported a hypothesis about the necessity to include the ingestion of radionuclides by marine organisms into the radioecological assessment.

The EFMARE project activity has planned to continue for two years:

The first year (2014):

Models developing and purchasing necessary input data, preliminary calculations and evaluation of influence of the modelling improvement.

- The present description of the bioaccumulation process is based on the use of constant concentration rates/factors. This approach can be significantly improved by involving a food web modelling approach which is particularly important during the initial dynamic phase of an accident when no equilibrium conditions exist.

- Development and implementation of the bioaccumulation process into the models as well as improvement of the models and comparison with previous results has been planned as most important part of the EFMARE activity in 2014.

- The time of an accident can be a significant factor for the evaluation of the radioecological consequences. This feature can be also implemented into compartment models. Implementation of the seasonality can be significant for many Nordic coastal sea areas, because their complex hydrodynamics often show a substantial seasonal variability. Evaluation of the seasonality with following implementation into the models is another task for the EFMARE project activity in 2014.

The second year (2015):

- Summary evaluation of consequences of severe radioactive releases to Nordic marine environment. Evaluation of the environmental sensitivity of the Nordic marine regions (Final Report of the activity).

- Evaluation of the dispersion of radionuclides in water and sediment phases with following effective dose calculation via marine food will be performed on the basis of the improved version of the computer codes from the national institutes (Hydrodynamic model from University of Iceland, VTT's Detra-code and NRPA compartment model) and will include improvement of the present models and description of accident scenarios by modelling of seasonality, by modeling of radionuclides bioaccumulation in marine organisms and modelling of biota movements, if necessary.

- Corroboration and validation of the improved models will be performed on the basis of provide comprehensive measuring data for the Nordic marine environment.

The present Interim Report provides a statement of the project after the year 2014 and includes description of the improvements of the modelling approaches, models and calculation results after the first phase of the project.

2. Improvements and achievements in modelling of radionuclides dispersal.

2.1. Temporal variability of pollutant dispersal in Icelandic Waters – a numerical case study (University of Iceland).

Maritime accidents can lead to a large variety of environmental threads. From oil slicks at the sea surface to dangerous material deposited at the sea floor, from dispersed molecules to drifting containers. Once an accident has happened the competent authorities will try to determine the risks for the ambient ocean area, particularly if the accident has happened in a coastal, economically important zone like the Icelandic waters. A crucial part of this risk assessment is the forecast of the particular pollutant's dispersal. Traditionally, estimated or assumed mean ocean current fields are used for these computations. However, meanwhile we obtained, based on refined measurements and numerical ocean simulations more information about the flow fields and found many indications of much more variable ocean dynamics than previously expected. The question arises whether and, if so, how this variability should be considered in those dispersal estimations. In this study we therefore examine the temporal variability of a fictive pollutant's dispersal in Icelandic waters with a set of numerical experiments based on the flow fields of an operational hydrodynamic model.

2.1.1. Experimental Setup

We selected the position 66.5°N, 25°W, northwest of Iceland within Denmark Strait as the location of a fictive accident. The ocean depth here is around 170 m which indicates that it is above the Icelandic continental slope. We assume a temporal constant source of

pollution which is evenly spread throughout the whole water column. This pollution is simulated by the gradual release of 5000 particles during a time period of 3 months. I.e. the particle initial positions is randomly chosen at 66.5°N±0.125°, 25°W±0.25° in a depth between 0 and 170 m. Thereafter, the particles' passive drift with the ocean currents, including a parameterized random walk referring to non-resolved turbulence, is simulated based on the data given by the hydrodynamic model CODE (Logemann et al. 2013).
The temporal range of these three-months experiments cover the four seasons, i.e. from 1 January to 31 March, from 1 April to 30 June, from 1 July to 30 September and from 1 October to 31 December. These four seasonal experiments are repeated for 10 different years: from 2004 to 2013. Hence, an overall number of 40 experiments were performed.

2.1.2. Results

In order to analyse the simulated particle drift pattern we used the 5000 particle positions (latitude, longitude) at the end of each experiment and converted these into a continuous "particle density" field. Therefore, we counted the number of particles in a 5 nm (9.26 km) radius around each point of a spherical matrix with a 1' resolution (fig. 1). Hence, the "particle density" describes the probability to find a particle at a given position. It can be also interpreted as the concentration of a pollutant emitted at the source position (point "S" in fig. 1).

All 40 experiments show a mainly eastward particle drift. However, also a south-westward drift onto the East-Greenland shelf can be detected (results of simulations can be found in the Appendix 1).

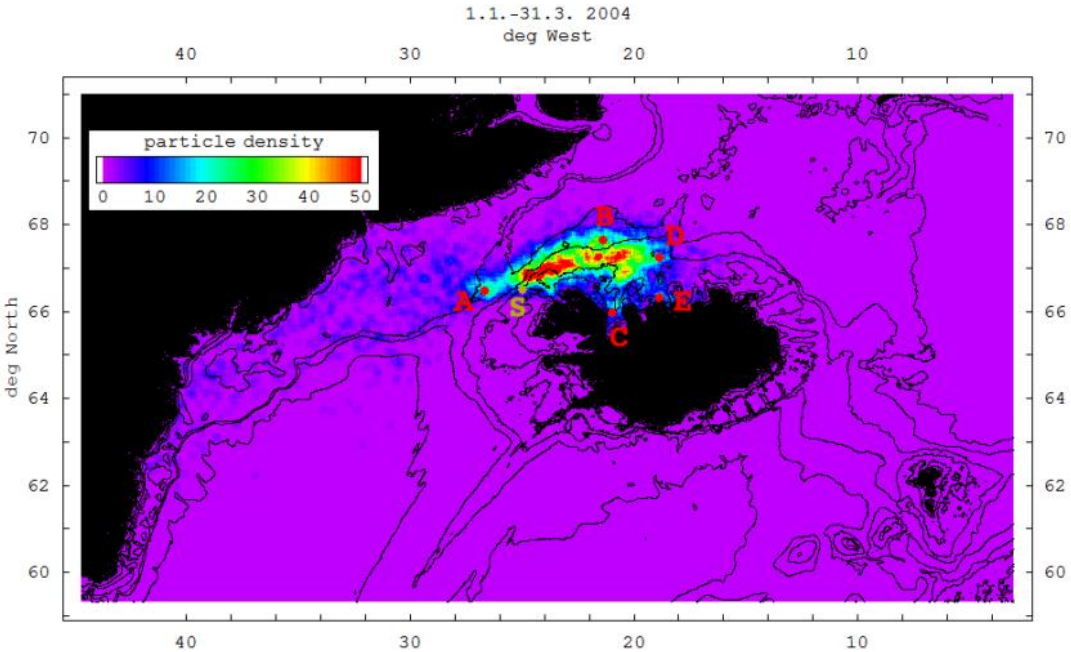

Fig. 1: Particle density at the end of the winter 2004 simulation. The point denoted with "S" shows the source position. The points "A", "B", "C", "D", and "E" denote the stations where time series were constructed.

Figure 1 shows the positions of five stations – A, B, C, D, E – where we extracted the particle density at the end of each experiments, this way obtaining five time series (tab. 1). The five time series show a generally high variability with values between 0 and 70 (figs. 2 – 6).

Table 1: Positions and depth of the five stations where the particle time series were extracted.

Station	Latitude (°N)	Longitude (°W)	Depth (m)
A	66.4833	26.7000	506
B	67.6500	21.3667	703
C	65.9833	20.9500	178
D	67.2333	18.8667	460
E	66.3167	18.8667	172

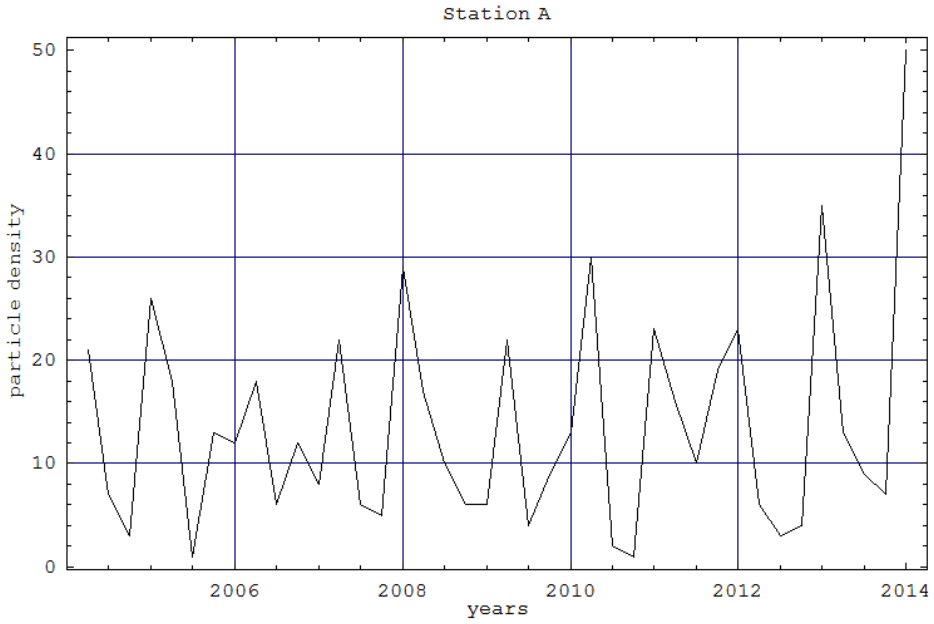

Fig. 2: Particle density time series at station A.

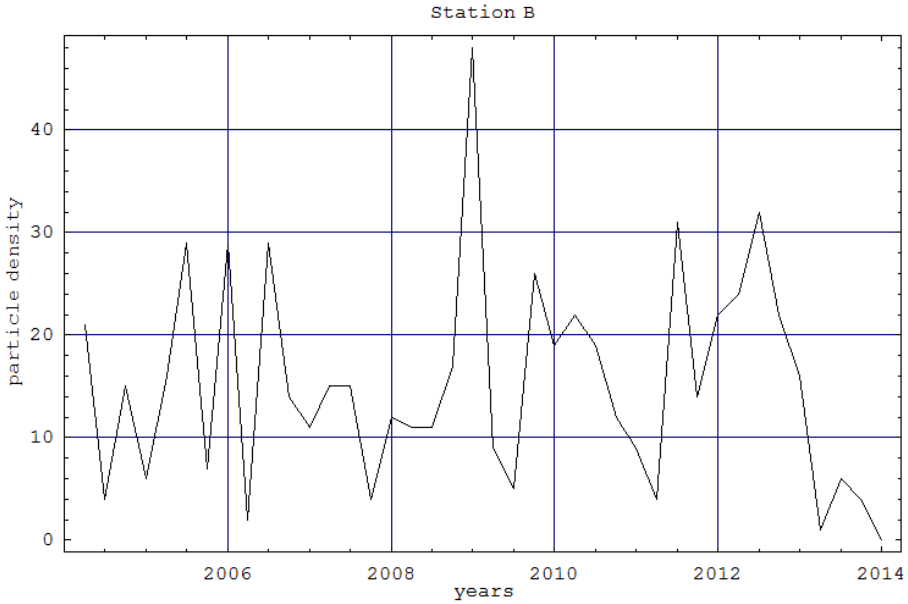

Fig. 3: Particle density time series at station B.

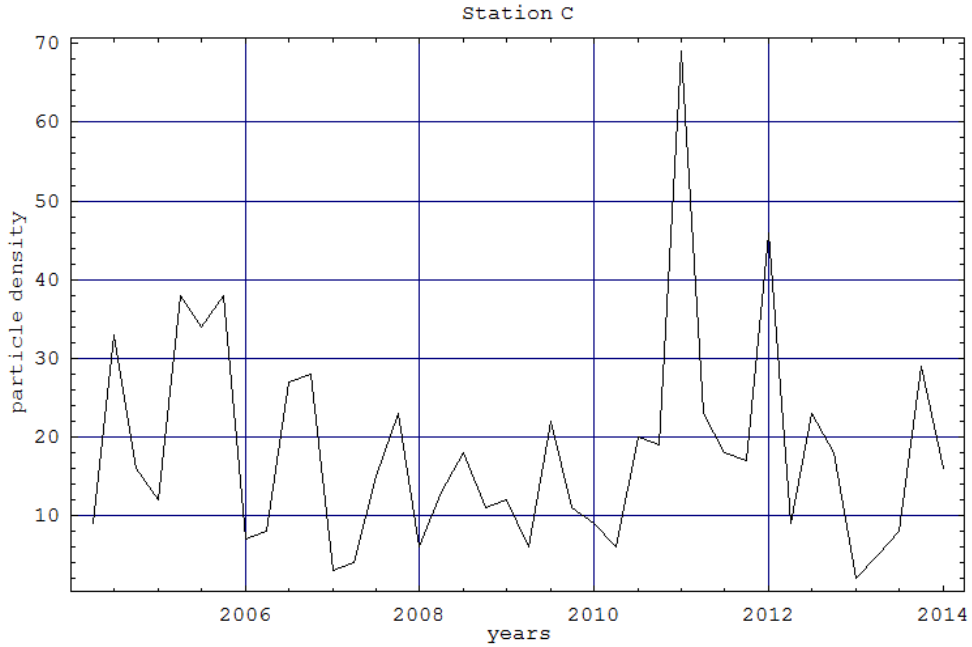

Fig. 4: Particle density time series at station C.

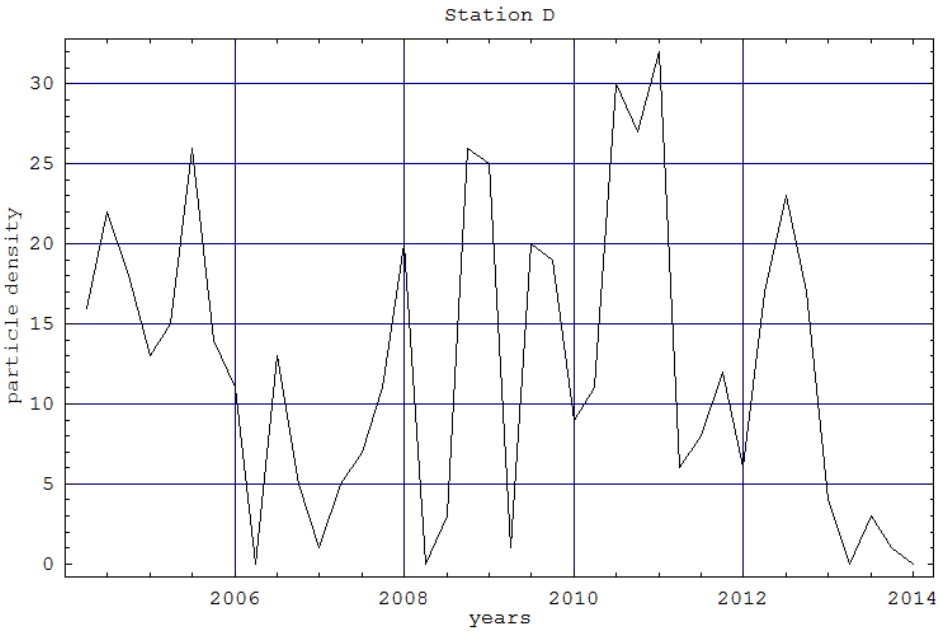

Fig. 5: Particle density time series at station D.

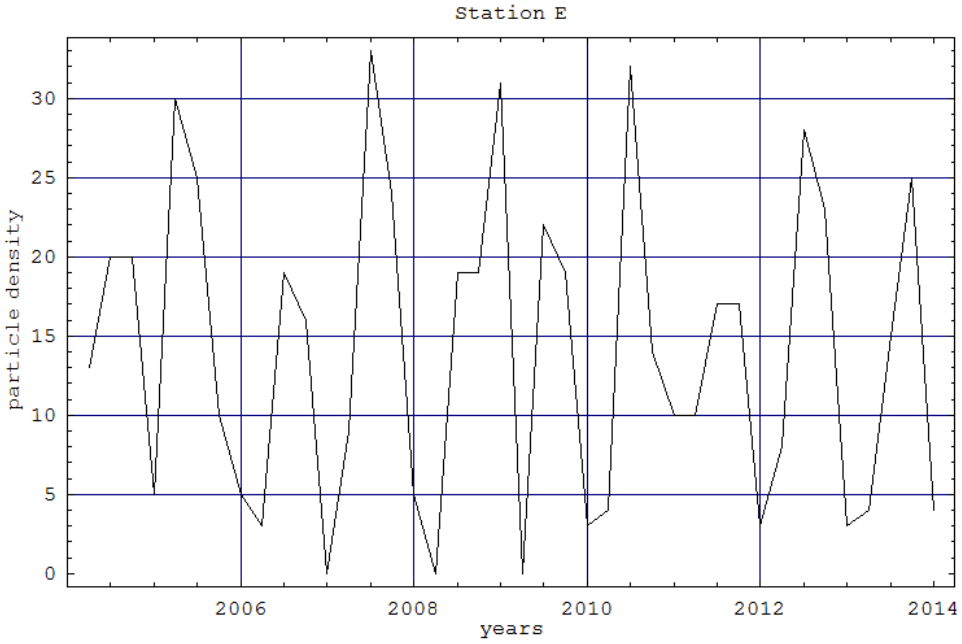

Fig. 6: Particle density time series at station E.

2.1.3. Discussion

The principal feature of the simulated pollutant dispersal is the eastward drift with the North Icelandic Irminger Current (NIIC), a flow of relatively warm and salty Atlantic Water northwards through Denmark Strait and further eastwards over the North Icelandic shelf. Therefore, at the end of the three-month simulation, the majority of the particles is found over the northern shelf between 25°W and 15°W.

The other pathway of particles, which is less established but equally persistent, leads to the south-west onto the East Greenland shelf. Here, even larger distances compared to the NIIC path are achieved, down to the southern tip of Greenland at 60°N. The explanation for this path is the turbulent entrainment of some particles near the source point into the southward flowing East Greenland Current. Between this cold and less saline current of polar origin and the Atlantic Water east of it exists an oceanic front, the Polar Front, and the dynamics involved explain the long distances reached by the particles. Another pathway, finally also leading to Greenland is an entrainment from the NIIC north of Iceland into the counter-directed North Icelandic Jet which carries the particle back to Denmark Strait into the southward flowing Arctic and Polar waters there.

However, though the eastward and the westward path are very persistent, we found large differences of the dispersal pattern among the individual 40 experiments (figs. A1 – A39). A striking example of this are the summer 2013 (fig. A38) and the autumn 2013 (fig. A39) experiment showing very different results, i.e. a strong westward transport during the first and a strong eastward transport during the latter period.

In order to analyse the dispersal's temporal variability we have constructed time series of the final particle density at five stations (A, B, C, D, E) based on the results of the 40 experiments, i.e. with a temporal resolution of three months. The stations were chosen to detect either the western branch (A) or the eastern branch over different parts of the north Icelandic shelf (B, C, D, E).

The frequency spectra of these time series, i.e. their discrete Fourier transformations, are show in figures 7 to 11. All spectra show a rather even distribution of periods between three months and ten years. This reflects the fact that changes of the dispersal pattern mainly depend on chaotic mesoscale atmospheric and oceanic fluctuations, i.e. on barotropic and baroclinic instabilities which in fact are highly likely to occur within the frontal areas west and north of Iceland where the Arctic ocean/atmosphere climate zone borders the sub-polar.

Only at station A and E a sharp maximum at the period of one year, i.e. a clear seasonal signal can be detected. Here, the correlation between the pure seasonal signal and the complete time series is 0.67 for station A and 0.70 for station E (figs. 12 and 13) whereas the analog correlations for the station B (fig. 14), C and D are: 0.05, 0.25 and 0.33 respectively.

The seasonal signal at station A shows its maximum at the beginning of the year. We assume that the stronger wind field during autumn and winter causes higher turbulence north-west of Iceland and therefore an increased entrainment of particles into the southwards flowing East Greenland Current which finally carries them to station A.

However, the seasonal signal at station E shows maximum values at beginning of the summer, after a relatively calm period. Because station E is located close to the North Icelandic coast, we assume the coastal current to be responsible for the signal. This current is forced by the salinity gradient caused by river runoff, and this runoff shows a peak in spring caused by the annual snowmelt. Hence, the transport of the coastal current increases at that time, therefore entrains more particles from offshore waters and carries them to station E.

Returning to the initial question: How should a pollutant dispersal forecast be performed? Our results show that long-term mean or seasonal mean flow fields used for their computation in Icelandic waters can easily introduce substantial errors because of the temporal variability inherent to this system with its considerable proportion of chaotic behaviour.

For short-term forecasts, extending not longer than two weeks, flow fields extracted from the current data of operational ocean models like the CODE system used for this study should be used. If the forecast has to reach further the question arises of determining the best flow field approximation for this purpose. One way could be just the continuation of the atmosphere and ocean forecast run assuming the more sluggish ocean dynamics drift slower into unrealistic states than the atmospheric. Other approaches could use the simulated current state and keep it stationary during the forecast period. Maybe trends of the short term forecast could be included. Hence, a large variety of mathematical techniques and methods should be explored in future in order to be able to produce optimal pollutant dispersal forecasts for Icelandic waters.

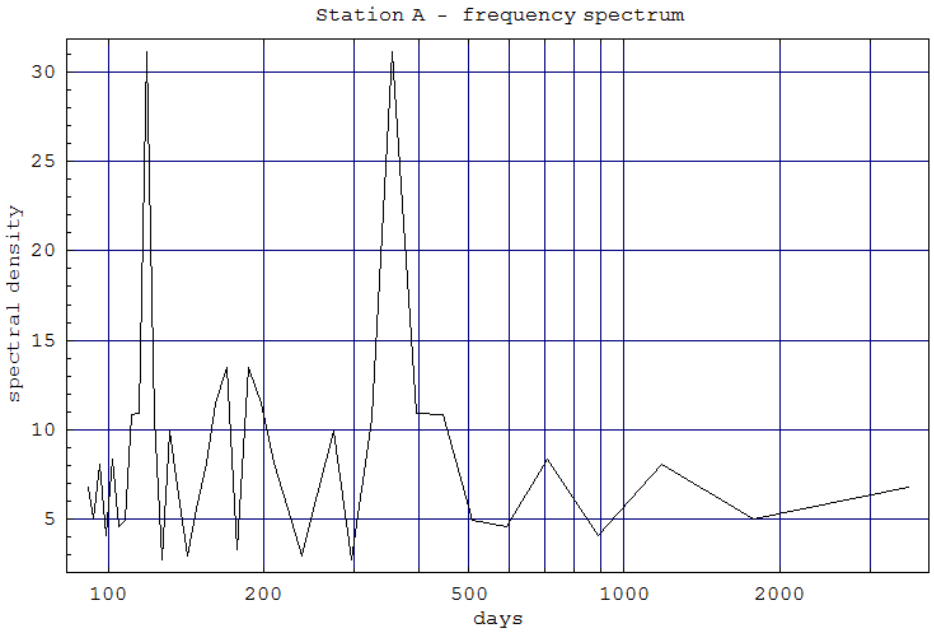

Fig. 7: Discrete Fourier transformation of the time series from station A.

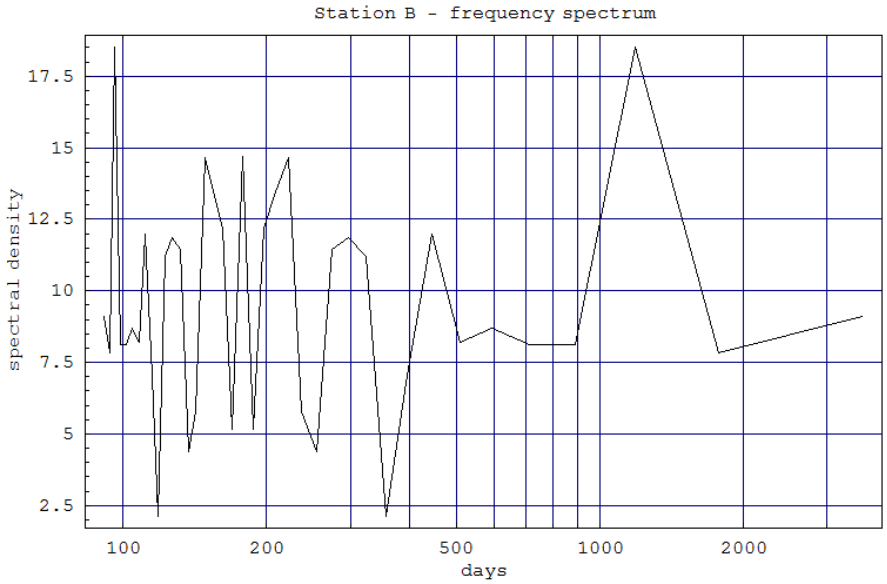

Fig. 8: Discrete Fourier transformation of the time series from station B.

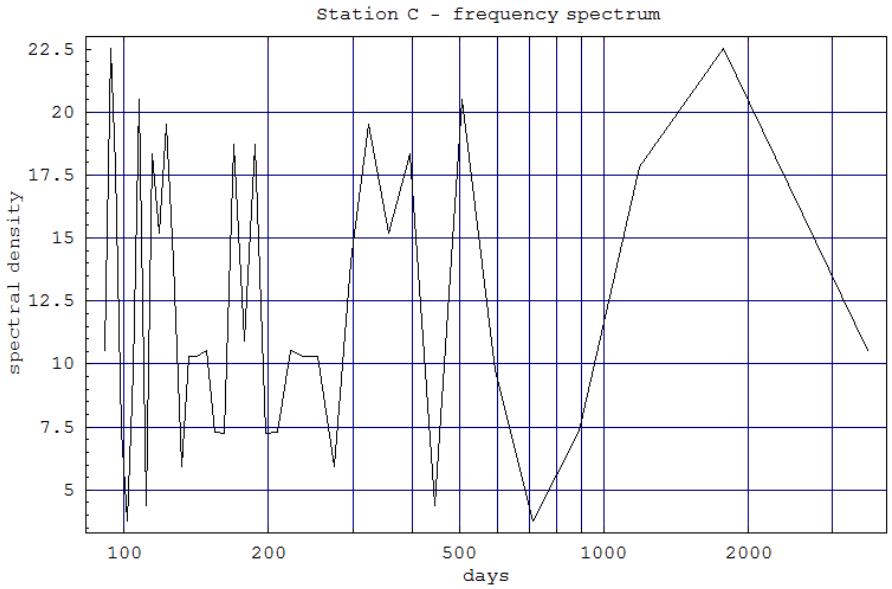

Fig. 9: Discrete Fourier transformation of the time series from station C.

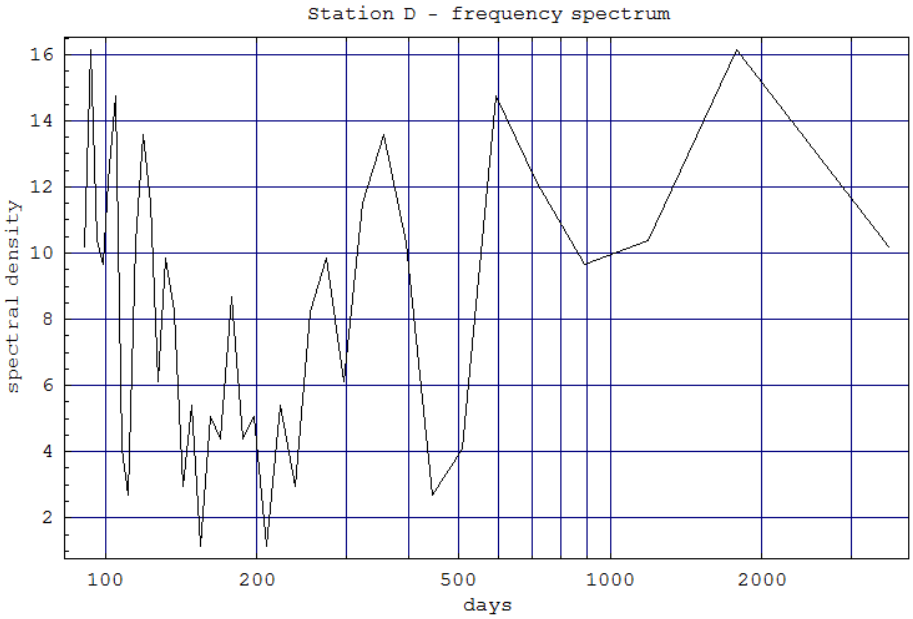

Fig. 10: Discrete Fourier transformation of the time series from station D.

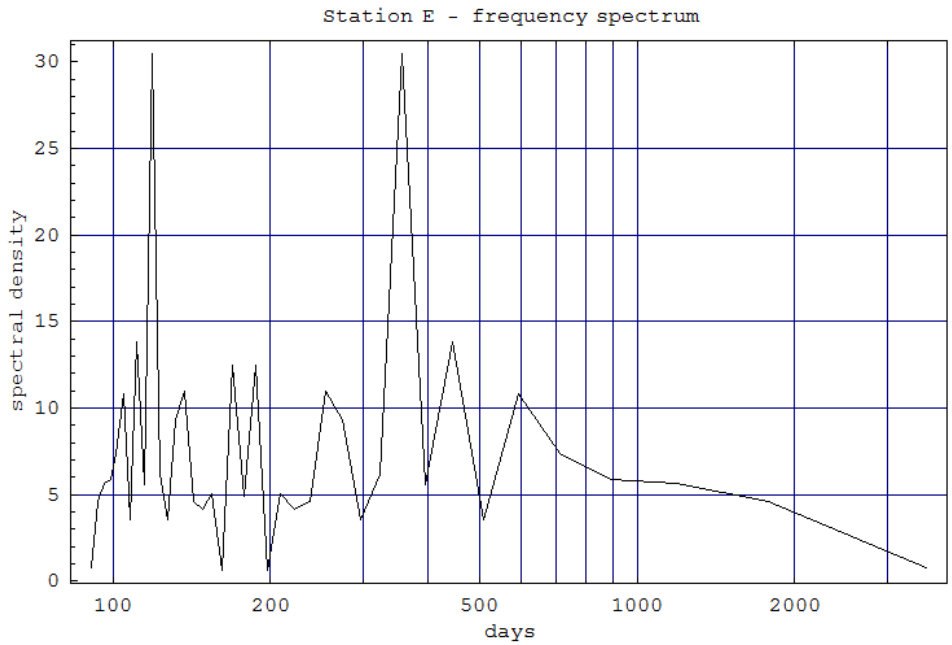

Fig. 11: Discrete Fourier transformation of the time series from station E.

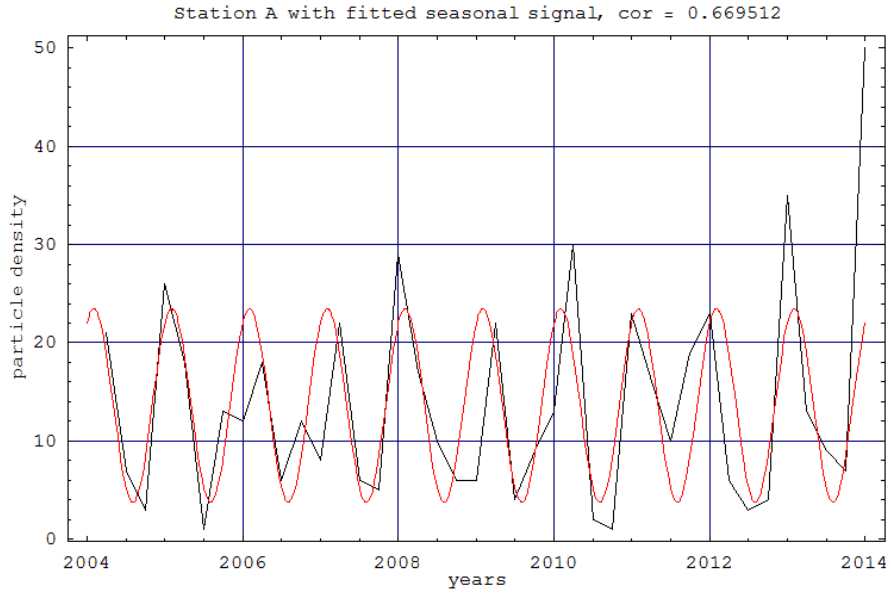

Fig. 12: Particle density time series at station A (black) and its mean seasonal signal (red).

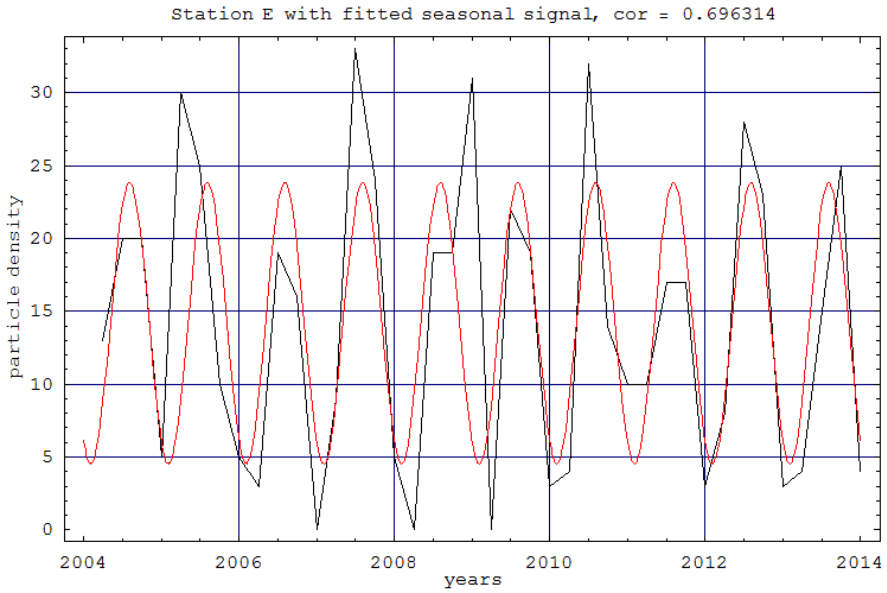

Fig. 13: Particle density time series at station E (black) and its mean seasonal signal (red).

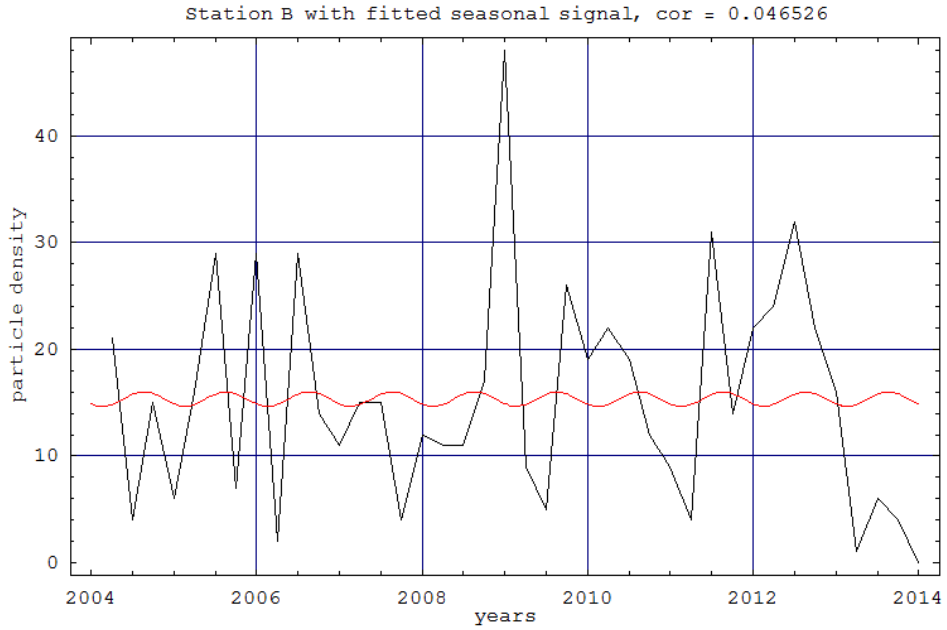

Fig. 14: Particle density time series at station B (black) and its mean seasonal signal (red).

2.2. An improvement of the NRPA dispersion model for the Baltic Sea.

The NRPA approach for box modelling includes terms describing the dispersion of radionuclides into oceanic space with time (Iosjpe et al., 2002; 2009). That is, the model considers that radionuclides cannot move from one box to another instantly. The model uses the times of availability for each box (the first times when box is open for dispersion of radionuclides). It is interesting to note that traditional box modelling is a particular case of the present approach when all times of availability are zero (more detailed description of the NRPA box approach is given in Appendix 2).

Under the course of the present project this modified approach was used for the description of the dispersion of radionuclides in the Barents Sea. Calculations show that this approach can significantly improve the modelling of the radionuclide dispersion, especially for the deep part of the Baltic Sea.

Sources for ^{137}Cs contamination of the Baltic Sea regions are shown in Figure 15 (COSEMA, 2014).

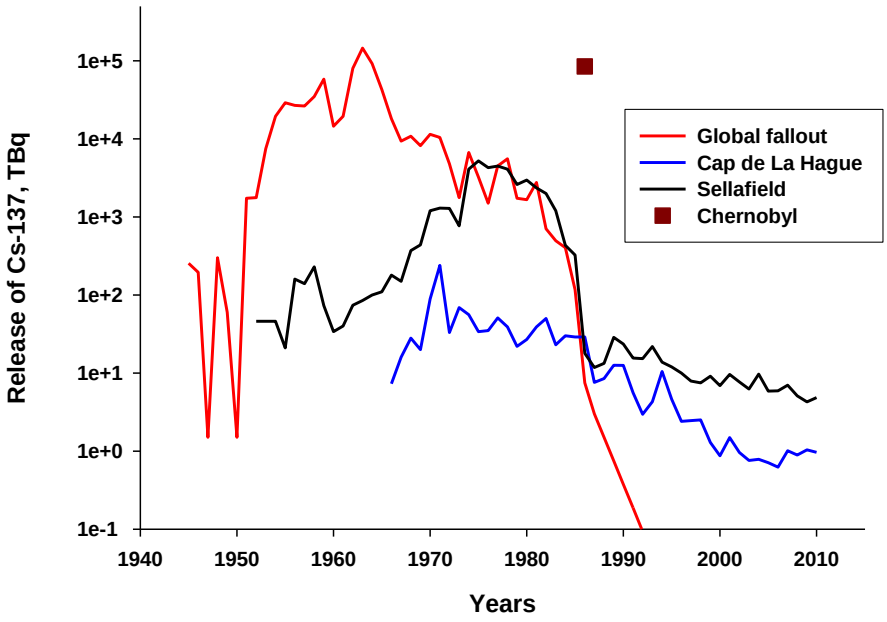

Figure 15. Sources of ^{137}Cs in the Baltic Sea.

Comparison of the ^{137}Cs concentration in the seawater for the Gulf of Finland and the deep waters of the Western and Eastern Baltic Sea are shown in Figures 16 and 17.

Figures 16 and 17 show the results of the model simulations for ^{137}Cs contamination compared with the experimental data (EC, 2000 and HELCOM, 1995). The circles and

quadrates show the average values, while the error bars show the minimum and maximum values of the experimental data. Figures 16 and 17 demonstrate that the model predictions are reasonably accurate.

It is a clear demonstration in Figure 17 that the NRPA box modelling modified approach can significantly improve the accuracy of the simulation of the radionuclide dispersion.

A good correlation between the results of model simulations of the ^{137}Cs concentration in seawater with the experimental data for the Gulf of Finland, provides a good opportunity for further testing of the bioaccumulation model.

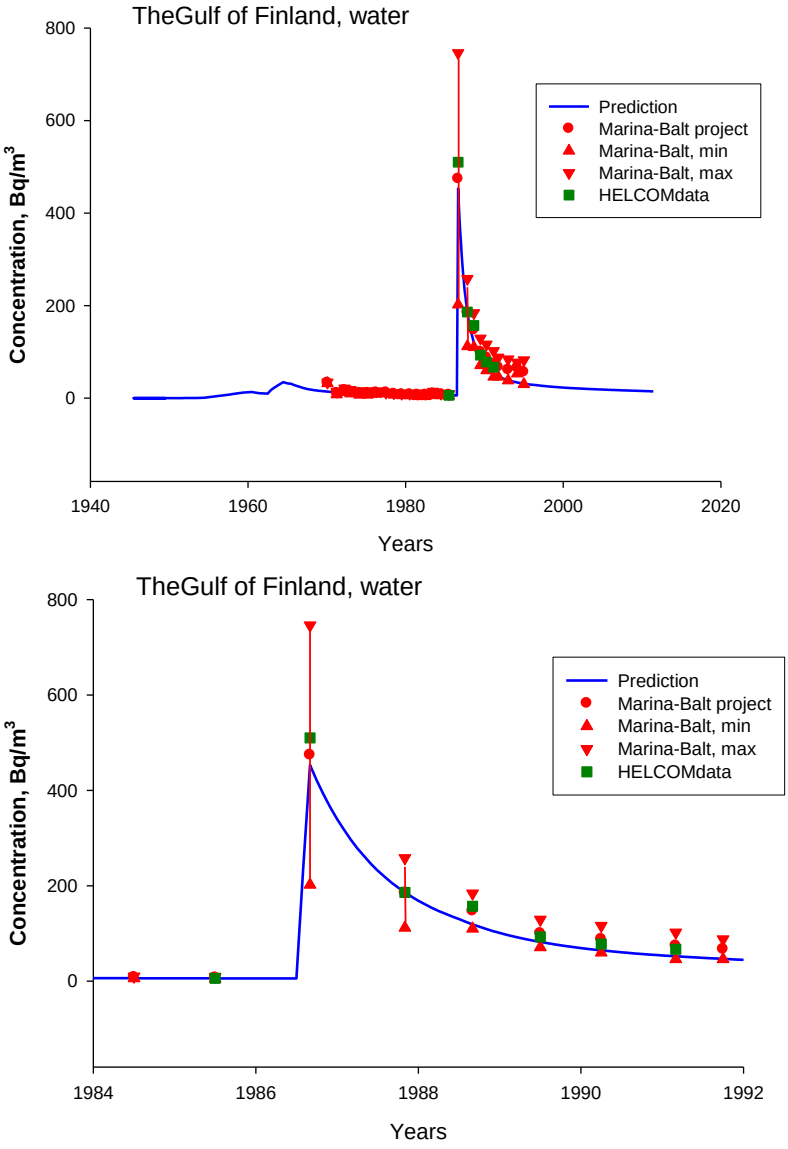

Figure 16. Comparison of the prediction of the concentration of ^{137}Cs in sea water with experimental data for the Gulf of Finland from 1945 (top) and for the Chernobyl accident (bottom).

Results of calculation outlined in Figures 17 clearly indicate potential significance of the modified approach for box modelling of consequences of discharges of radionuclides into marine areas in comparison to traditional modelling.

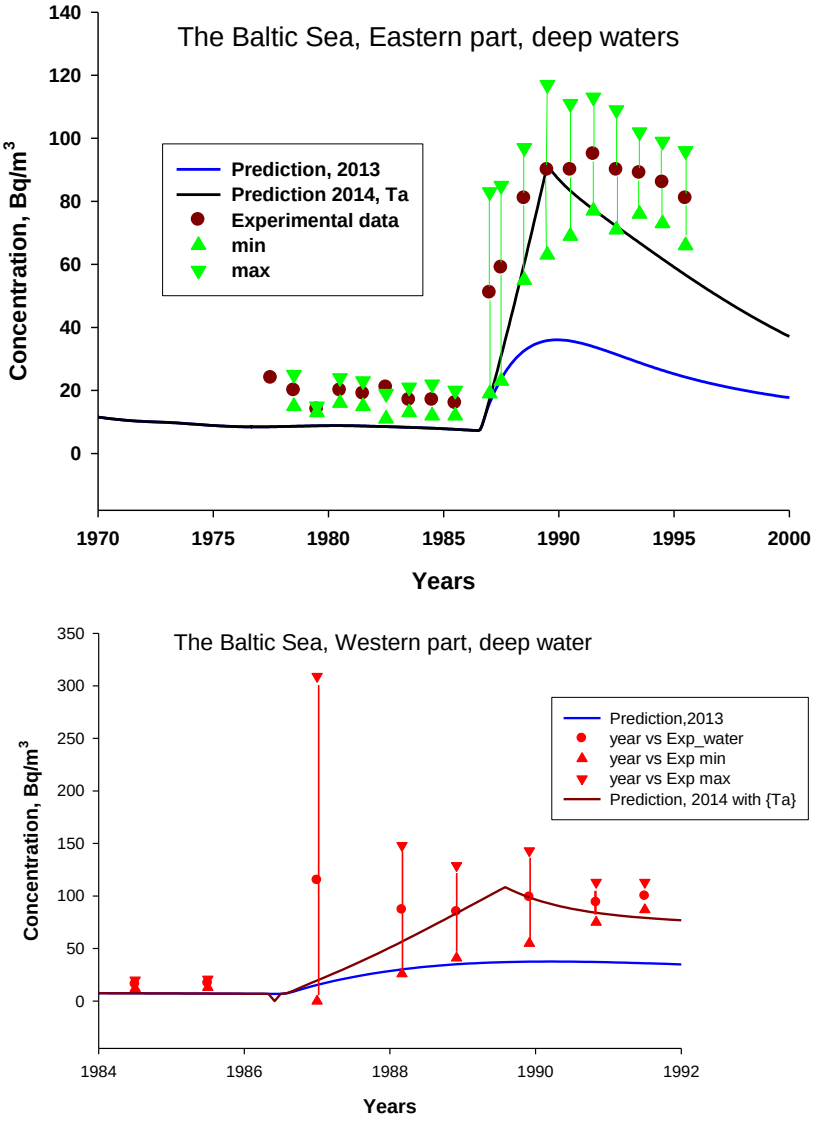

Figure 17. Comparison modified (2014, Ta) and traditional approches with experimental data for deep waters of the Baltic Sea after the Chernobyl accident.

3. Bioaccumulation modelling

3.1. Development and implementation of the bioaccumulation process into the NRPA box model

The NRPA model uses a modified approach for box modelling with non-instantaneous mixing of radioactivity in the marine environment (Iosjpe et al., 2002, 2009; see also Appendix 2 of the present report). The model includes site-specific information for the compartments, advection of radioactivity between compartments, sedimentation, diffusion of radioactivity through pore water in sediment, resuspension, mixing due to bioturbation, particle mixing, a burial process for radionuclides in deep sediment layers and radioactive decay. The contamination of biota is calculated from the known radionuclide concentrations in filtered seawater in the different water regions on the basis of constant concentration factors /ratios (CF approach). Doses to man are calculated on the basis of seafood consumption, in accordance with available data for seafood catches and assumptions about human diet in the respective areas. Dose to biota is calculated on the basis of radionuclide concentrations in marine organisms, water and sediment, using dose conversion factors.

3.1.1. Modelling of the bioaccumulation process

Analysis of existing models (Thomann, 1981; Heling et al., 2002; Brown et al., 2004; Vives i Batlle et al., 2008; Maderich et al., 2013) showed that the models developed by Thomann (1981) and Brown et al. (2004) are most suitable as a basis for the EFMARE project, though some improvements may be needed.

Figure 18 shows the schematic of the biokinetic model from (Thomann, 1981) with an additional assumption about possibility of uptake of radionuclides via zooplankton for large fish (the blue arrow in Figure 18).

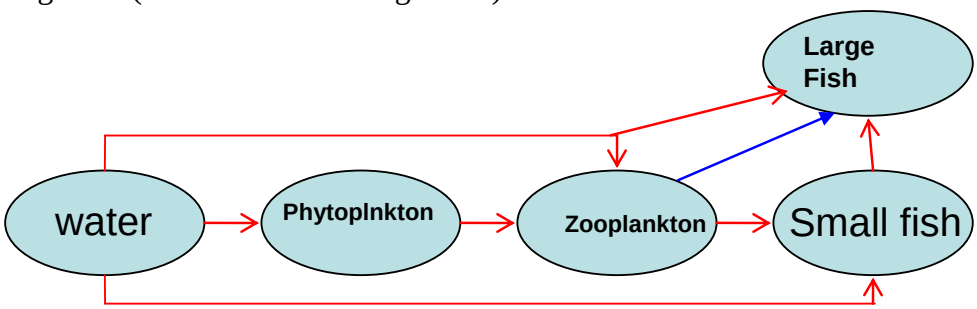

Figure 18. Schematic of the biokinetic model used in the present report.

The system of equations for the biokinetic model can be described by the following expressions:

$$\frac{dC_i^{(tl)}}{t} = AE_i \cdot IR_i \cdot C_{i-1}^{(tl)} + k_{u,i} \cdot C_w - C_i^{(tl)} \cdot k_{e,i} \quad (1)$$

Here $C^{(tl)}_i$ and $C^{(tl)}_{i-1}$ – concentrations of radinuclide in trophic levels ”i” and ”i-1”,
C_W – concentration of radionuclide in water column,
AE_i – the assimilation efficiency for trophic level "i",
IR_i – ingestion per unit mass for trophic level "i",
$k_{u,i}$ – rate of the direct uptake of activity from water column for trophic level "i",
$k_{e,i}$ – the excretion rate for trophic level "i".

Comparison of the activity concentration in biota between a constant concentration factor approach and a biokinetic modelling approach is shown in Figure 19. Calculation of the concentrations of radionuclides for phytoplankton is based on concentration factor approach. Results of the implementation of the kinetic model for bioaccumulation processes into the NRPA box model clearly demonstrated that there is a significant difference between the kinetic modelling approach and the approach based on constant concentration factors, especially during the initial time of dispersion. After some time an equilibrium is established, which can be successfully described by a constant concentration ratio approach.

Using constant concentration factors to describe the process of bioaccumulation has several advantages. Due to the large number of studies, there is a database for concentration factors for many radionuclides, which significantly exceeds the information about biokinetic coefficients needed for more complex models. Furthermore, biokinetic modelling is a more sophisticated method, when compared to the constant concentration ratio approach. Therefore, it often requires more detailed and specific data about the concentraion of radionuclides in the marine enviroment, and this data may sometimes be difficult to measure or predict. This is because we often need to work with a complex marine environment which is contaminated by many different sources of pollution, many of which interact with each other.

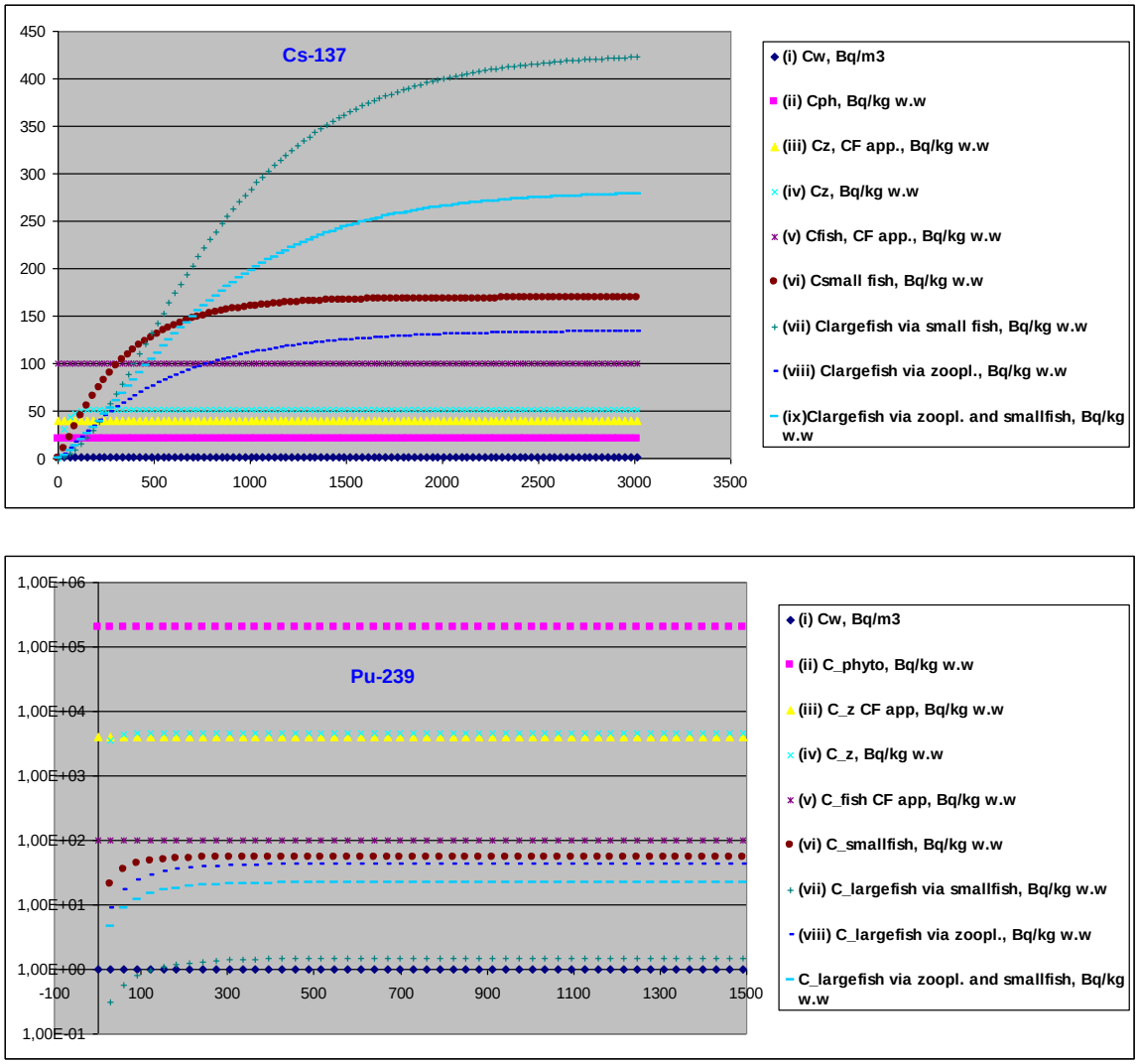

Figure 19. Comparison of the concentration of radionuclides in biota for both the constant concentration factor approach and the biokinetic modelling for ^{137}Cs (top) and ^{239}Pu (bottom) with the concentrations: (i) in water, (ii) in phytoplankton (iii) in zooplankton with concentration factor approach, (iv) in zooplankton with biokinetic modelling, (v) in fish with concentration factor approach, (vi) in small fish with biokinetic modelling, (vii) in large fish with biokinetic modelling and uptake via water and small fish, (viii) in large fish with biokinetic modelling and uptake via water and zooplankton, (ix) in large fish with biokinetic modelling and uptake via water, zooplankton and small fish.

Figure 20 indicates the complexity of some marine regions. In these regions the radionuclide dispersion after atmosphere fallout, as well as releases from European and Russian nuclear facilities, has occurred for decades. The concentration factors/ratios for these marine environments are shown in Figure 21 (experimental data was collected by Fróðskaparsetur Føroya and Technical University of Denmark over the course of the

EFMARE project). Results of calculations indicate variability of the concentration factors/ratios for the same fish in different environments and times, as well as between different species. At the same time, the results can be described by concentration ratio 100 for fish (IAEA, 2004) with a relatively large variability, approximately a factor of 4. No clear patterns of change of concentration factor can be determined; rather we must speak about the influence of random factors related to the complexity of the migration of radionuclides in the marine environment and prolonged exposure to various sources of pollution.

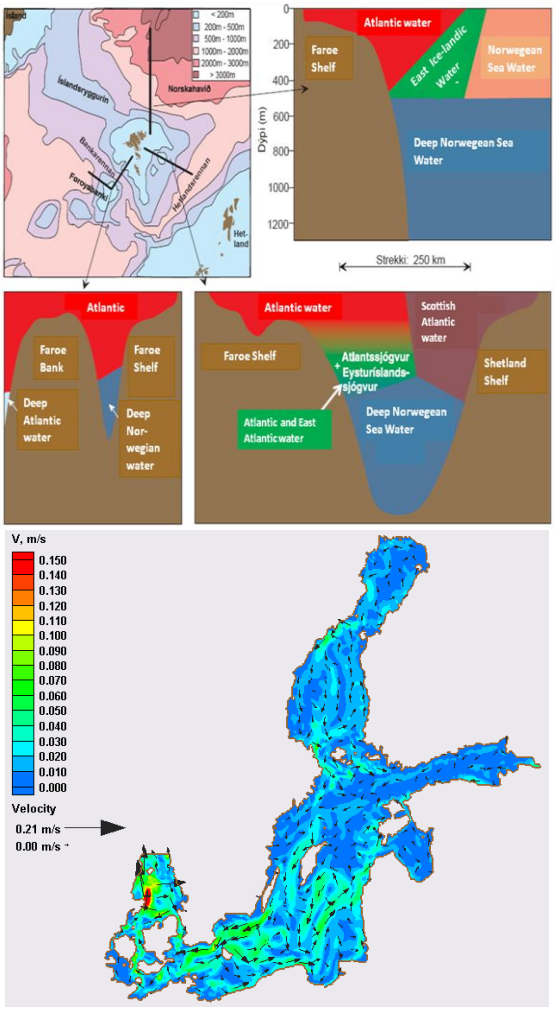

Figure 20. Water mass distribution for the Faroe region (top; Hansen, 2000) and water currents for the Baltic Sea (bottom)

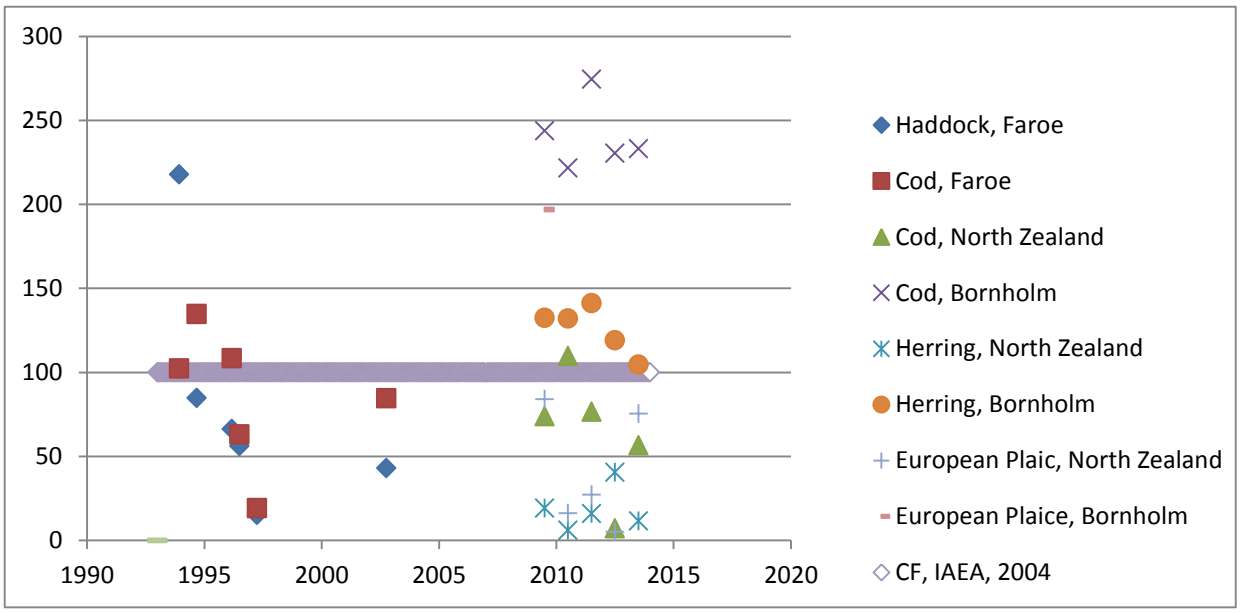

Figure 21. ^{137}Cs ratios (CR) for fish for the Faroe and the Denmark coastal waters.

On the other hand, Figure 20 shows that the bioaccumulation described using biokinetic modeling can be very important in an accidental release of radionuclides. This conclusion is confirmed by studies of the consequences of the Fukushima accident (Maderch, 2013). Because precisely such accident scenarios are considered in the EFMARE project, the biokinetic sub-model has been tested by applying it to the consequences after the Chernobyl accident in the Gulf of Finland (the Gulf of Finland was chosen due to the good correlation between the predicted and the measured data for ^{137}Cs concentration in the water, making it highly suitable to test the biokinetic submodel).

Results of biokinetic modelling approach were compared with experimental data on the basis of an improved version of the NRPA box model for the Baltic Sea (see Figure 22). Blue and red lines in Figure 22 correspond with concentrations in water and fish (with concentration factor approach), correspondently. Therefore, these plots have the same shape. Biokinetic modelling describes the "delay" with the changing of concentration of radionuclides in water. It is a clear demonstration that the dynamic modelling of the bioaccumulation processes provides a more correct description of the concentration of radionuclides in biota (up to an order of magnitude) and, therefore, these results support one of the main ideas of the EFMARE project, namely that the biokinetic modelling approach is important when evaluating the consequences after accidental releases of radionuclides into a marine environment.

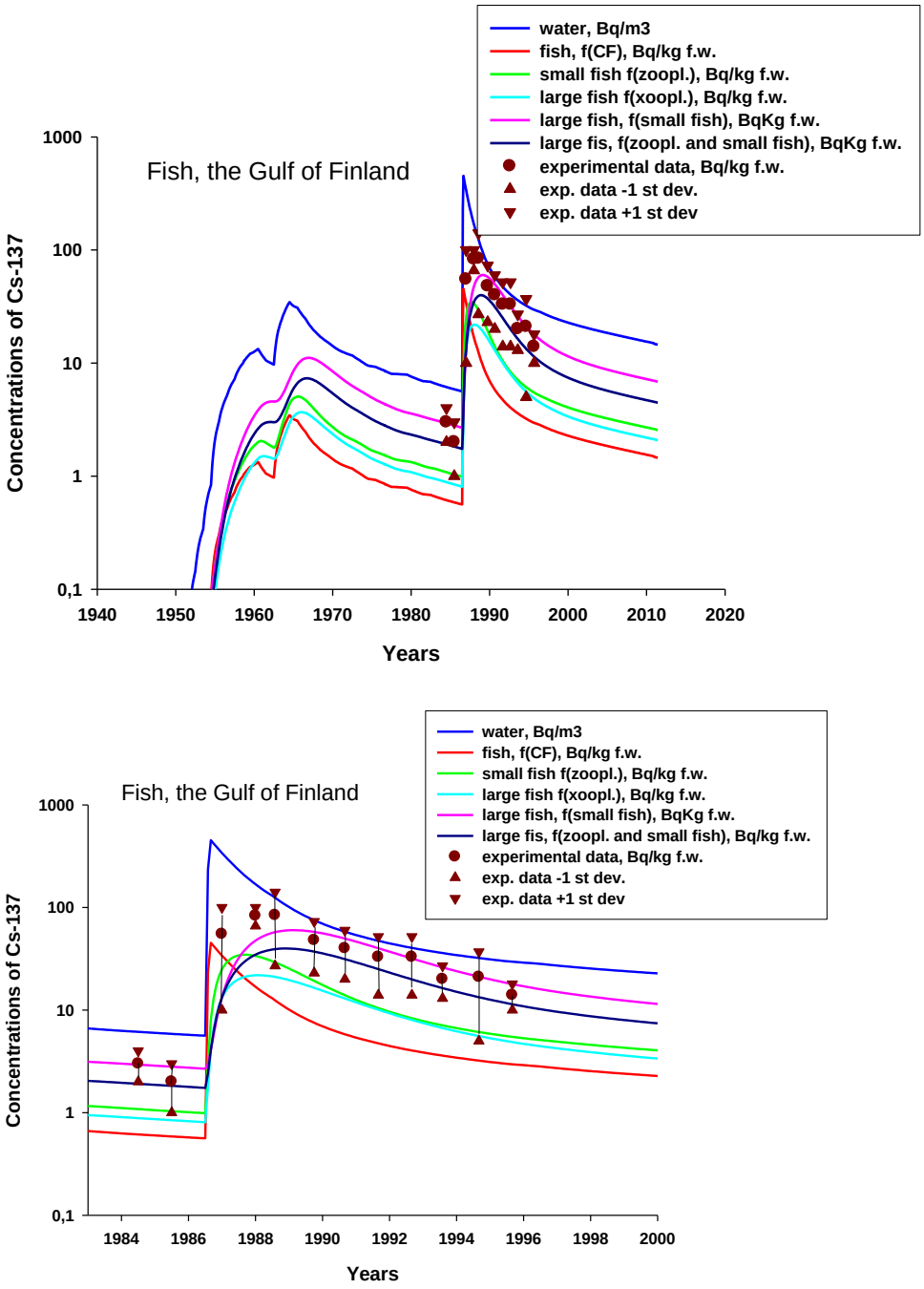

Figure 22. Comparison of the prediction of the concentration of ^{137}Cs in fish with experimental data for the Gulf of Finland for both the constant concentration factor approach and the biokinetic modelling from 1945 (top) and for the Chernobyl accident (bottom).

It is important to note that knowledge about biokinetic coefficients based on habitat, ingestion of food, diet and excretion of activity for studied species are crucial information for biokinetic modelling. Useful information can be found in Brown et al. (2004), Vives i Batlle (2008), Yankovich et al. (2010), Maderch et al. (2013) and Appendix 3 of the present report (data in Appendix 3 was collected by University of Gothenburg over the course of the EFMARE project).

3.2. Development and implementation of the bioaccumulation process into the DETRA computer code (Technical Research Centre of Finland)

The conceptual compartmental dispersion model consists of dynamic models for marine basin and for fish food chain (Figure 23). The DETRA computer code can be applied for radionuclides transfer analyses as well as for parametric sensitivity studies.

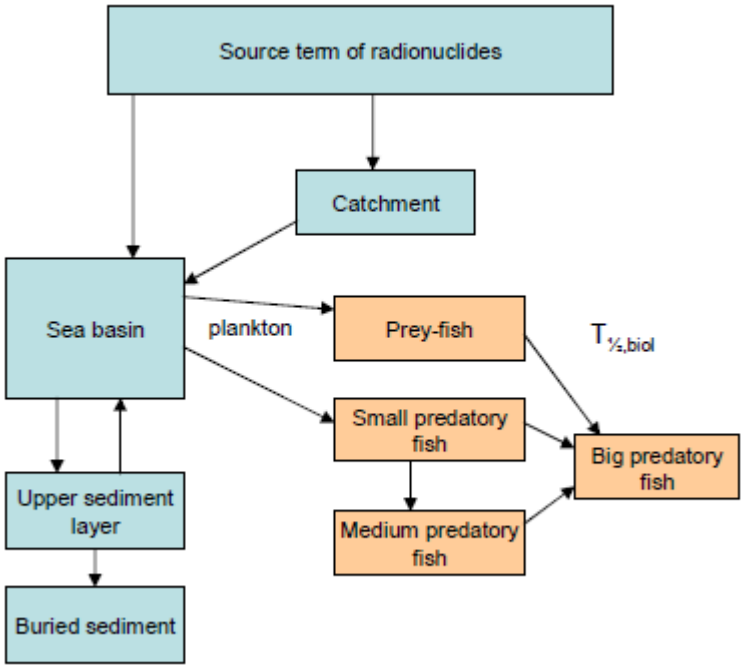

Figure 23. Conceptual bioaccumulation model for marine environment.

In each of the model compartments sufficient homogenization of concentrations are assumed to be reached. Radionuclides transfer between compartments is modelled with convective carry flows of water and suspended sediment material. As consideration of radionuclides transfer, the main flow rates are generally related to seawater turnover and to sedimentation of suspended material from seawater to the bottom sediment layer. Additionally, there are also other important transfer mechanisms like erosion from catchment towards sea. This erosion is caused by runoff and by wind induced erosion

where radionuclides are first dispersed into the atmosphere, and further deposited onto seawater.

Mechanisms which tend to dilute (e.g. seawater turnover) or on the other hand mechanisms which tend to concentrate (e.g. radionuclides uptake to fish or sedimentation) are essential factors when estimating the build-up of radionuclide concentrations in various parts of the considered marine ecosystem. Additionally, the element specific sorption characteristics determine the final distribution between water phase and solid matter. Therefore, the soluble nuclides are mainly carried with seawater and strongly sorbing nuclides are mainly carried with solid matter (sedimentation).

The concentration responses of prey fish occur quite soon, whereas the maximum of predatory fish concentration can be obtained in later phase (Figure 24). Predatory fish is placed later in the food chain than prey fish and biological half-life of predatory fish is longer compared to prey fish (Table 1).

Table 1. Biological half-lives estimates for Cesium in fish types.

Fish type	$T_{½,\,b}$ (day)
Prey fish	50 … 100
Predatory fish (small)	150 … 250
Predatory fish (big)	200 … 400

Although Figure 24 presents dynamic behaviour of fish concentrations in lake environment, similar type of temporal behaviour will be obtained also for marine ecosystem concentrations. Development of bioaccumulation model for marine ecosystem with relevant parameter values, is in progress.

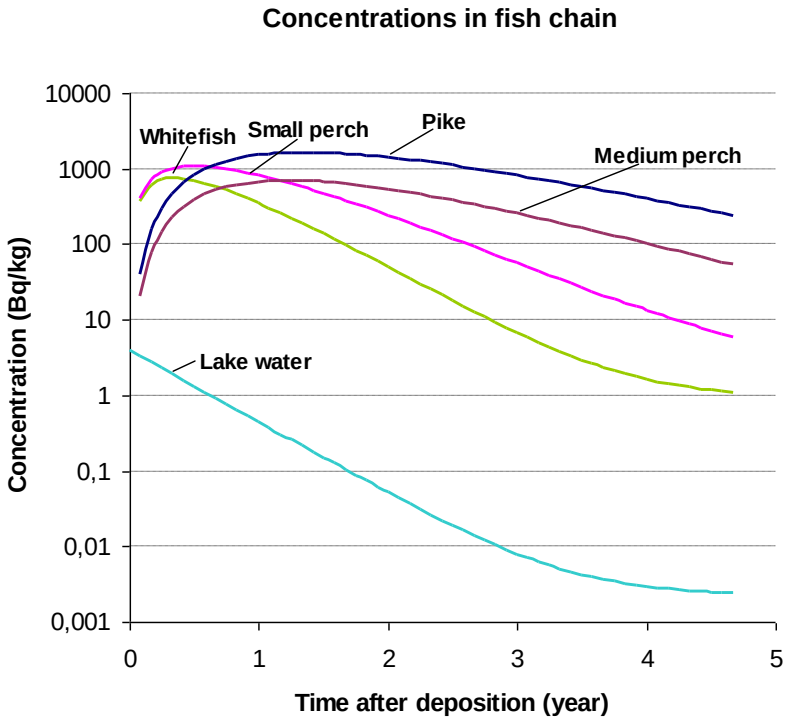

Figure 24. Dynamic behaviour of fish type concentrations after a 10 kBq(Cs-137)/m^2 deposition to lake environment (relatively small water basin).

4. Severe accident source term and consequences

4.1. The Baltic Sea (DETRA computer code)

The revised source term estimates for Fukushima accident indicate lower release fractions e.g. for Cesium (UNSCEAR 13-85418). New estimates for direct release in Fukushima to the ocean is 3 to 6 PBq and indirect release to the ocean 5 to 8 PBq for Cs-137. With the Fukushima reactors inventories this corresponds to a release fraction of about 2% for Cesium.

Considering the new reference release fraction data for severe accident, updated consequences for a 3000 MWth release case to the Baltic Sea is calculated assuming conservatively Cesium release fraction of 5% to sea (Figure 25).

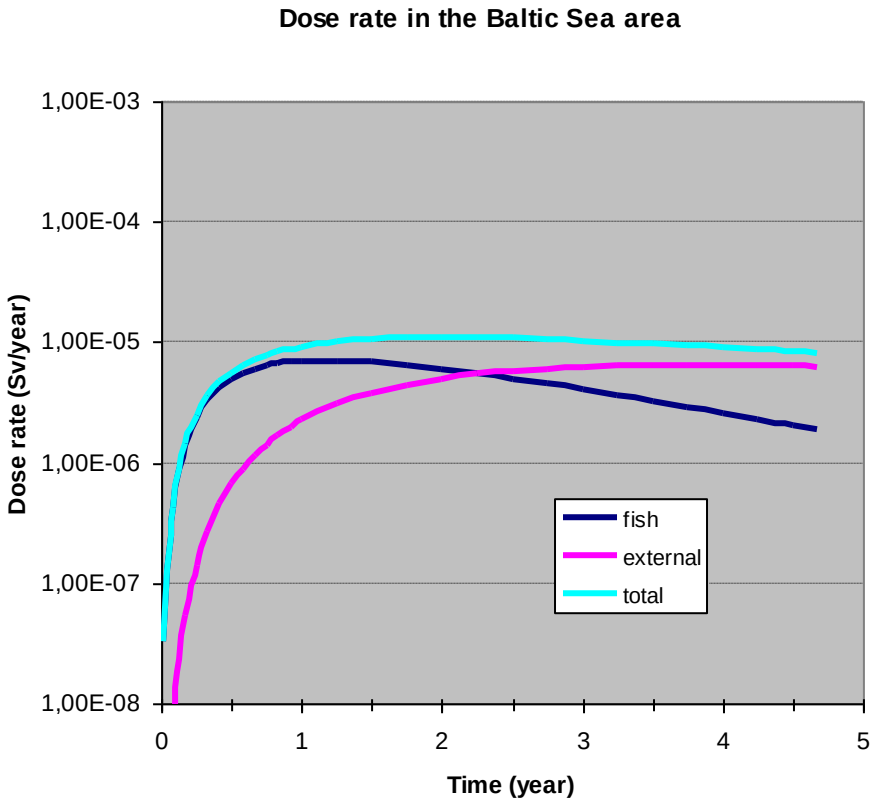

Figure 25. Individual dose rates after severe radioactive release to the Baltic Sea. Reactor power 3000 MWth, Cesium release fraction 5% of total inventory. Doses from fish consumption, external exposure from shoreline sediments and total dose rate, are presented.

Comparison of two release scenarios: release from the Finnish coast and release from the Swedish coast is presented in Figure 26 (Cs-137 concentrations in the Baltic proper after release). According to calculations, the concentration in the Baltic appear earlier in case of release from the Swedish coast. The maximum Cs-137 concentration in seawater is about 1 Bq/liter.

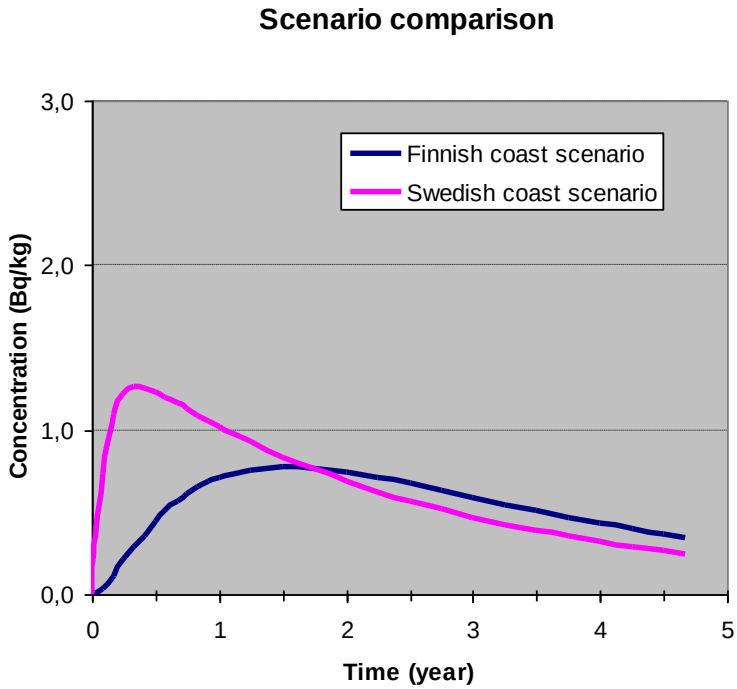

Figure 26. Comparison of estimated Cs137 concentrations in the Baltic sea between the 'Finnish coast' and the 'Swedish coast' release scenarios.

4.2. The Iceland coastal waters (NRPA regional box model COSEMA)

A release scenario for the hypothetical accident with a nuclear submarine in the Icelandic coastal waters is described in detail in (COSEMA, 2014). According to this scenario, about 25 PBq of ^{137}Cs was released into the marine environment. The dynamics of the releases of ^{137}Cs for ten years is shown in Figure 27.

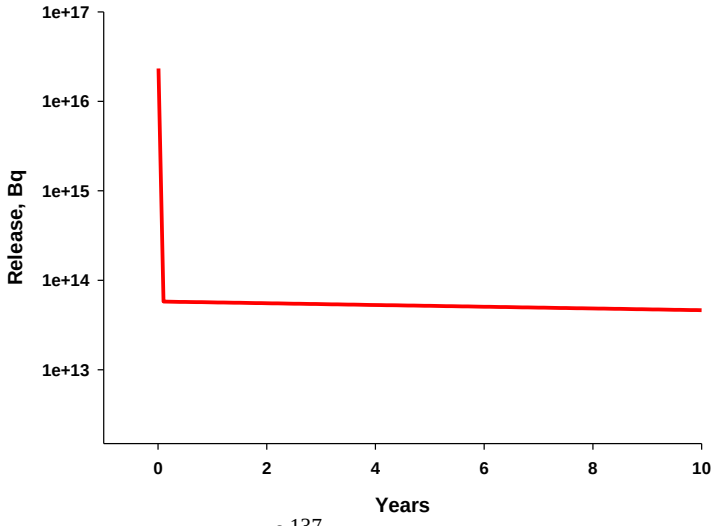

Figure 27. Release of ^{137}Cs into seawater

Figure 28 shows calculation of ^{137}Cs concentration (box 2, see Fig. A2.1, Appendix 2) in seawater and fish according to this scenario, corresponded to the accident location. Results in Figure 26 shows the same shape for the plots of concentrations for water with maximal value in initial time (a red line) and all kinds of fish (a green line), while use of the biokinetic model leads to another shape of plots with gradual increase and then decrease of the fish concentration similar to results in Figure 22 (blue and brown lines).

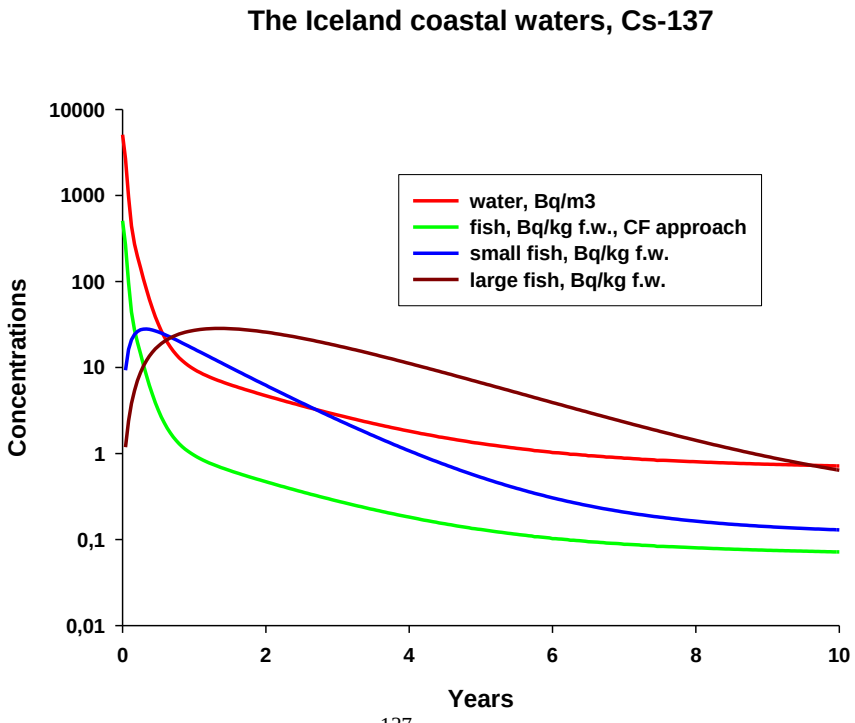

Figure 28. Concentrations of ^{137}Cs in seawater and fish.

The results of calculation of ^{137}Cs concentration with the constant concentration ratio approach lead to different dose distribution for the critical group (the group of high consumption of seafood) compared to the biokinetic modelling approach. Results in Figure 29 shows that when the concentration ratio approach is used, the maximum corresponded to the first year (26 μSv) and becomes almost insignificant in subsequent years. The use of the biokinetic approach for doses to the critical group for large fish, results in a distribution with the maximum dose corresponded to the second year (16 μSv), with slight decreases in subsequent years. At the same time, the total dose after ten years for the concentration ratio approach and for the biokinetic modelling approach are equal to 27 μSv and 60 μSv, respectively.

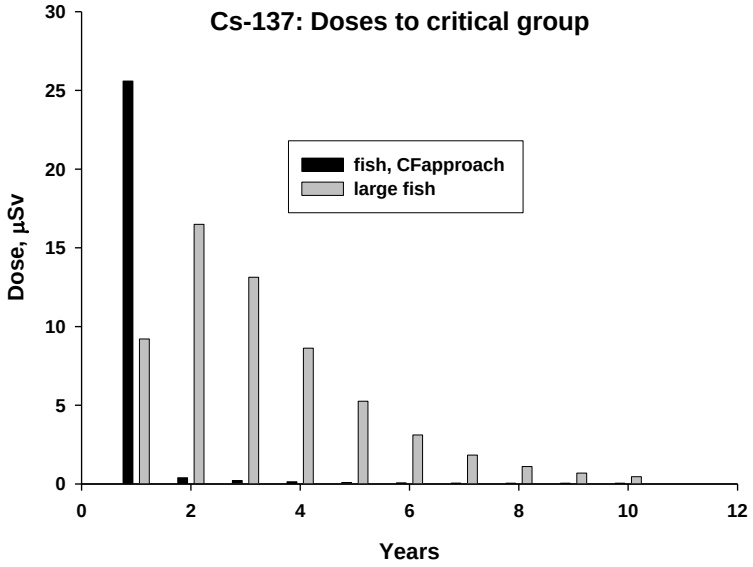

Figure 29. Doses the critical group from fish consumption.

5. Conclusions

Results of implementation of the kinetic model for bioaccumulation processes into the NRPA box model and the DETRA computer code clearly demonstrated that there is a significant quantitative difference between the kinetic modelling approach and the approach based on the constant concentration rates.

Results of modelling were compared with experimental data on the basis of improved version of the NRPA box model for the Baltic Sea. It is clear demonstration that dynamic modelling of the bioaccumulation processes can provide a more correct description of the concentration of radionuclides in biota and, therefore, these results support the main goal of the EFMARE project.

With a numerical case study the temporal variability of pollutant dispersal in Icelandic waters was demonstrated and discussed. The simulations, which contain a pollution source in Denmark Strait northwest of Iceland, are based on flow and turbulence fields provided by the CODE operational ocean model. The results show a spreading directed mainly eastwards over the north Icelandic shelf with the North Icelandic Irminger Current. Another path leads into the southward directed East Greenland Current. The dispersal into both branches shows a high inter-seasonal variability whereas the role of the seasonal signal is, at least in certain areas, only of minor importance. The results emphasize the necessity to use operational hydrodynamic ocean models in order to forecast pollutant dispersal in Icelandic waters.

The use of particle density can be used for comparison with simulations from the NRPA box model.

Study of the temporal variability of pollutant dispersal in Icelandic waters shows that simultaneous use of different models (eg hydrodynamic and box models) can significantly improve the description of dispersion of radionuclides in the marine environment.

The recalculation of the results for the NPP in the Baltic Sea region has been carried out based on corrected information concerning the source term from the Fukushima accident. It is shown that the concentration in the Baltic appear earlier in case of release from the Swedish coast. Preliminary results show that the maximum Cs-137 concentration in seawater is about 1 Bq/l.

References

Brown J., Børretzen P., Dowdall M., Sazykina T., and Kryshev I., 2004. The derivation of transfer parameters in the assessment of radiological impacts on Arctic marine biota. Arctic, 57, No. 3, 279-289.

COSEMA, 2014. Consequences of severe radioactive releases to Nordic marine environment. Final report for the NKS-B COSEMA activity 2013, Contract AFT/B(13)3.

EC (2000). The radiological exposure of the population of the European Community to radioactivity in the Baltic Sea, Marina-Balt Project. European Commission, Luxembourg, EUR 19200.

Hansen, B., 2000. Havið (*The Ocean*). ISBN: 99918-0-248-7. (In Faroese)

HELCOM, 1995. Radioactivity in the Baltic Sea 1984-1991. Baltic Sea Environment Proceedings 61, 182 pp.

Heling R., Koziy I., Bulgakov V., 2002. On the dynamic uptake model developed for the uptake of radionuclides in marine organisms for the POSEIDON-R model system. Radioprotection 37 (C1), 833-838.

IAEA, 2004. *Sediment distribution coefficients and concentration factors for biota in the marine environment.* IAEA Technical reports series no. 422. Vienna: International Atomic Energy Agency, IAEA.

Iosjpe, M., J. Brown & P. Strand, 2002. Modified approach for box modeling of radiological consequences from releases into marine environment, Journal of Environmental Radioactivity 2002, 60, 91–103.

Iosjpe M., M. Karcher, J. Gwynn, I. Harms, R. Gerdes and F. Kauker (2009). Improvement of the dose assessment tools on the basis of dispersion of the ^{99}Tc in the Nordic Seas and the Arctic Ocean. *Radioprotection*, vol. **44**, n^{o} 5, 531-536.

Logemann, K., J. Ólafsson, Á. Snorrason, H. Valdimarsson, and G. Marteinsdóttir (2013): The circulation of Icelandic waters – a modelling study, Ocean Sci., 9, 931-955, doi:10.5194/os-9-931-2013, 2013.

Maderch V., Bezhenar R., Heling R., G. de With, Jung K.T., Myoung J.G., Cho Y.-K., Qiao F., Robertson L., 2013. Regional long-term model of radioactivity dispersion and fate in the Fukushima Dai-ichi accident. Journal of Environmental Radioactivity 2013, www.elsevier.com/locate/jenvrad.

Thomann R.V., 1981. Equilibrium model of fate of microcontaminants in diverse aquatic food-chains. Canadian Journal of Fisheries and Aquatic Sciences 38:280-296.

UNSCEAR 2013 Report. Volume I, Scientific Annex A: Levels and effects of radiation exposure due to the nuclear accident after the 2011 great east-Japan earthquake and tsunami. UNSCEAR 13-85418.

Vives i Batlle J., Wilson R.C., Watts S.J., Jones S.R., McDonald., Vives-Lynch S., 2008. Dynamic model for assessment of radiological exposure to marine biota. Journal of Environmental Radioactivity 99, 1711–1730.

Yankovich T.L. et al., 2010. Whole body to tissue concentration ratios for use in biota dose assessments for animals. Radiat. Environ. Biophys. 49, 549-565.

Appendix 1. Graphics of particle density

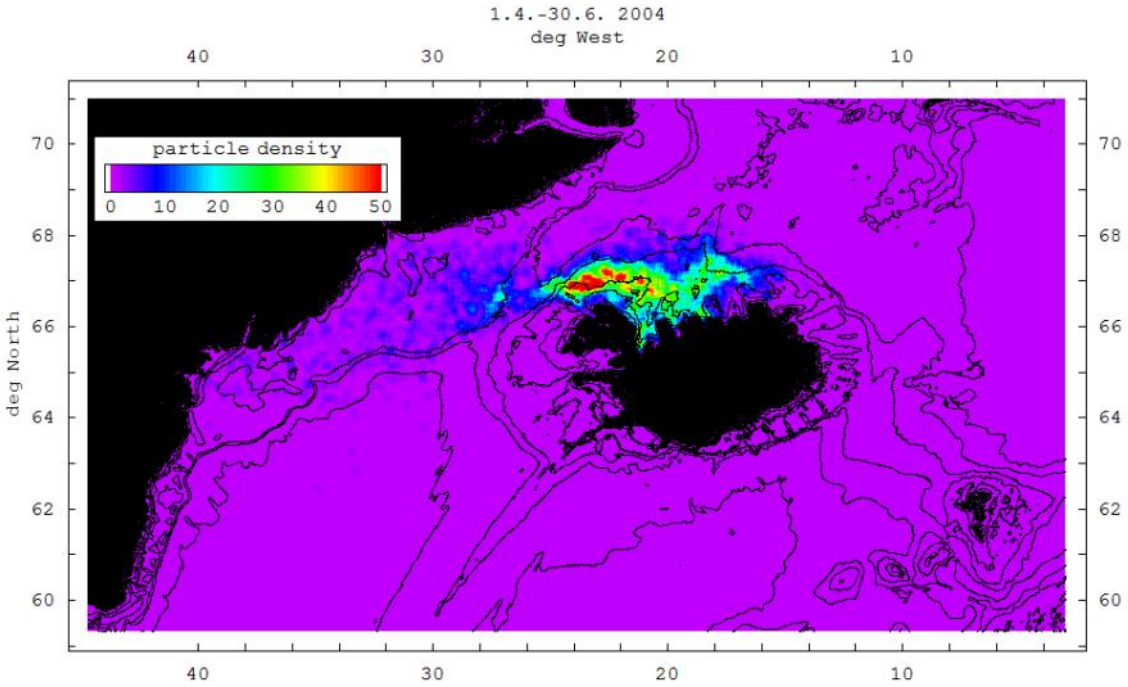

Fig. A1.1: Particle density at the end of the spring 2004 simulation.

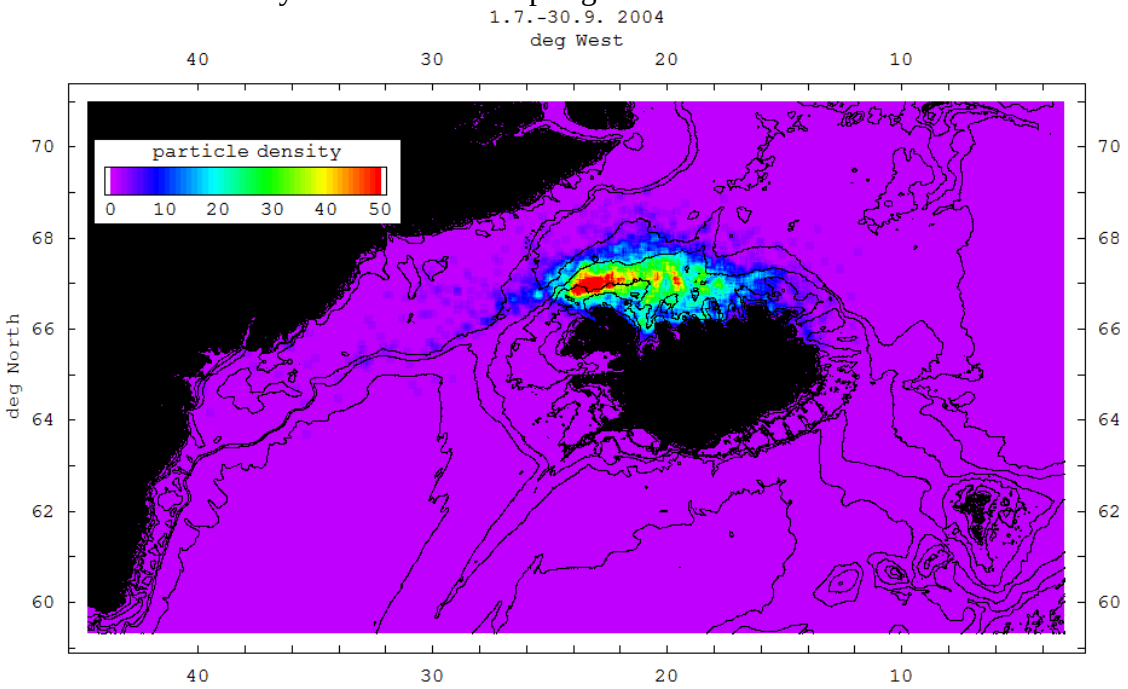

Fig. A1.2: Particle density at the end of the summer 2004 simulation.

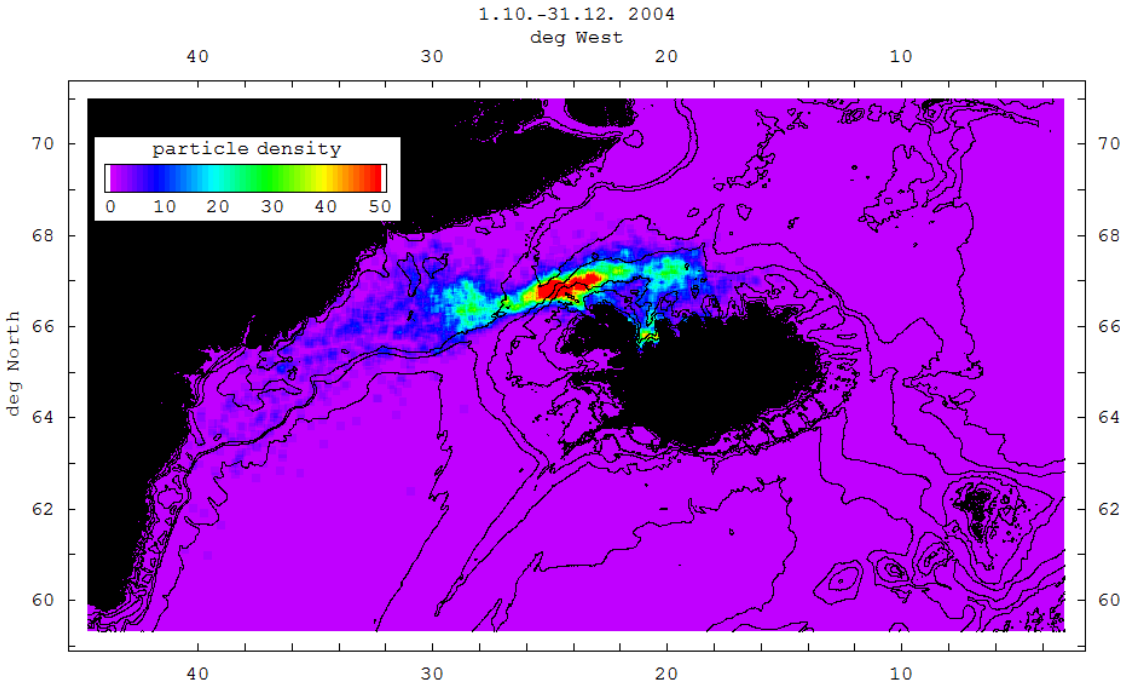

Fig. A1.3: Particle density at the end of the autumn 2004 simulation.

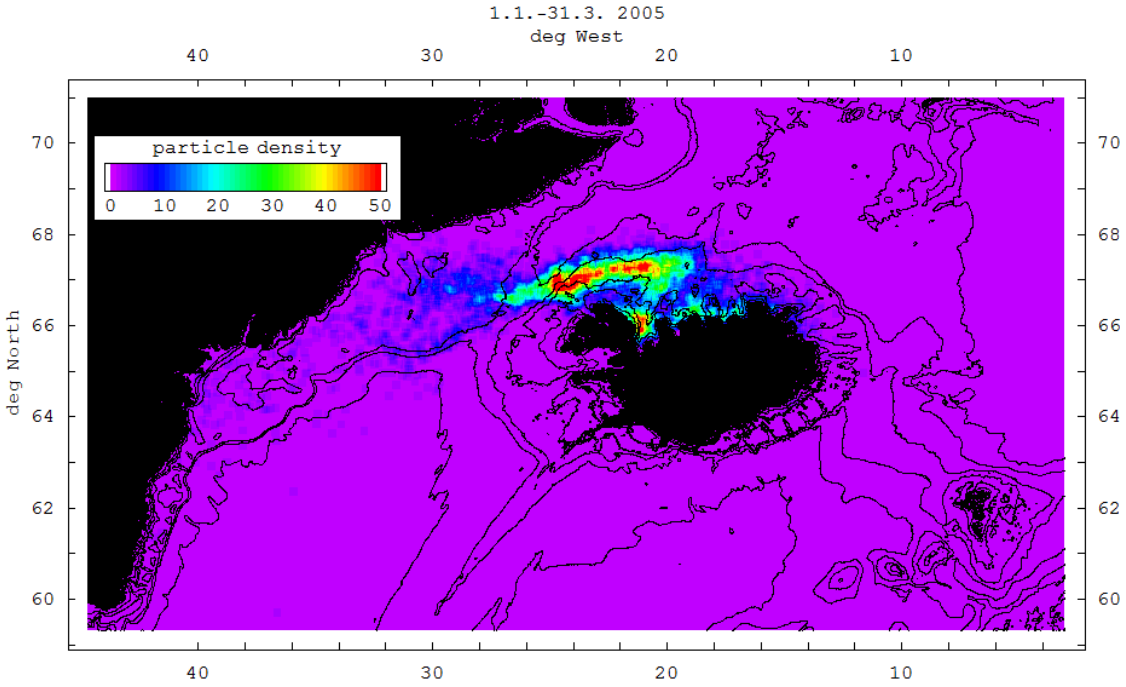

Fig. A1.4: Particle density at the end of the winter 2005 simulation.

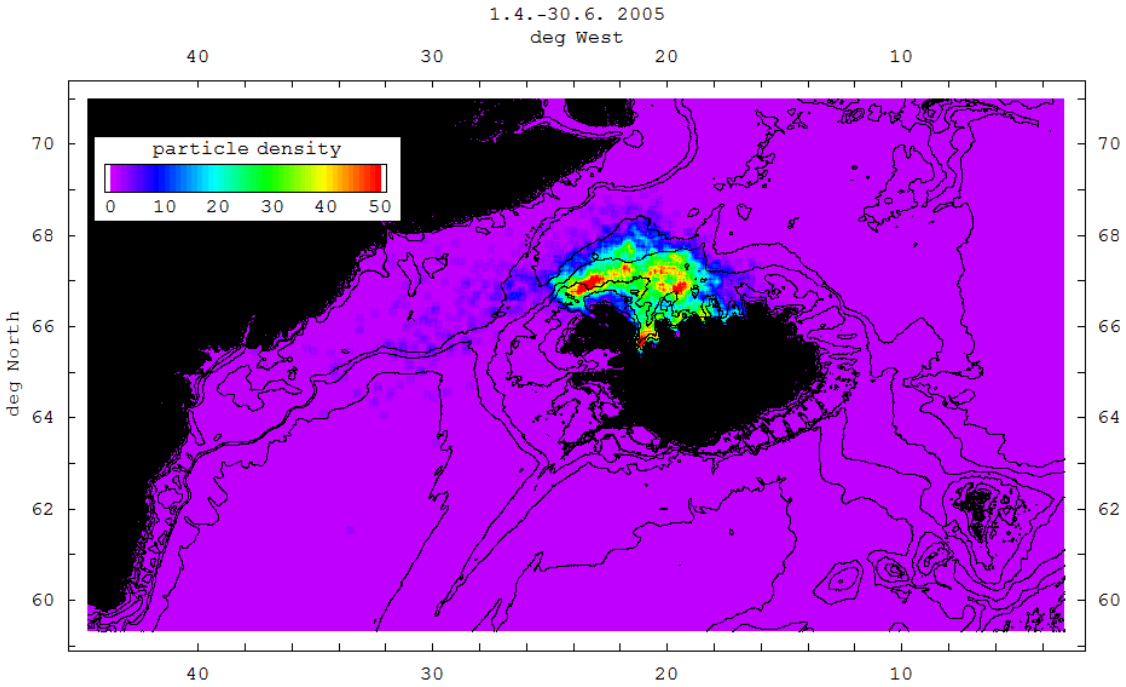

Fig. A1.5: Particle density at the end of the spring 2005 simulation.

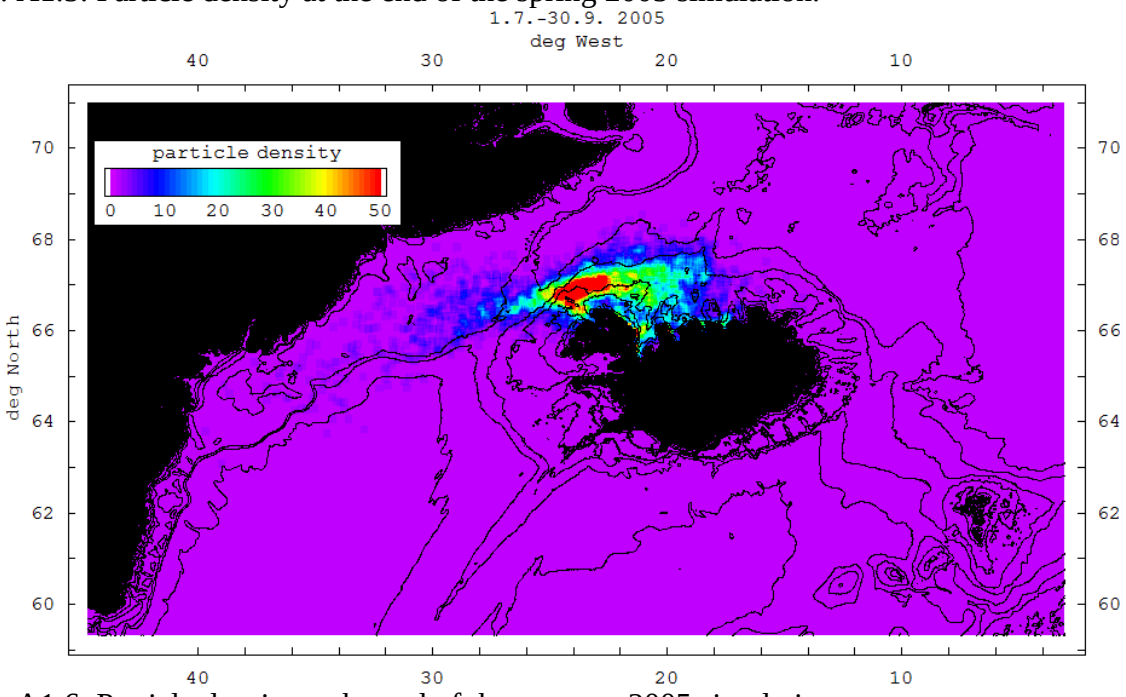

Fig. A1.6: Particle density at the end of the summer 2005 simulation.

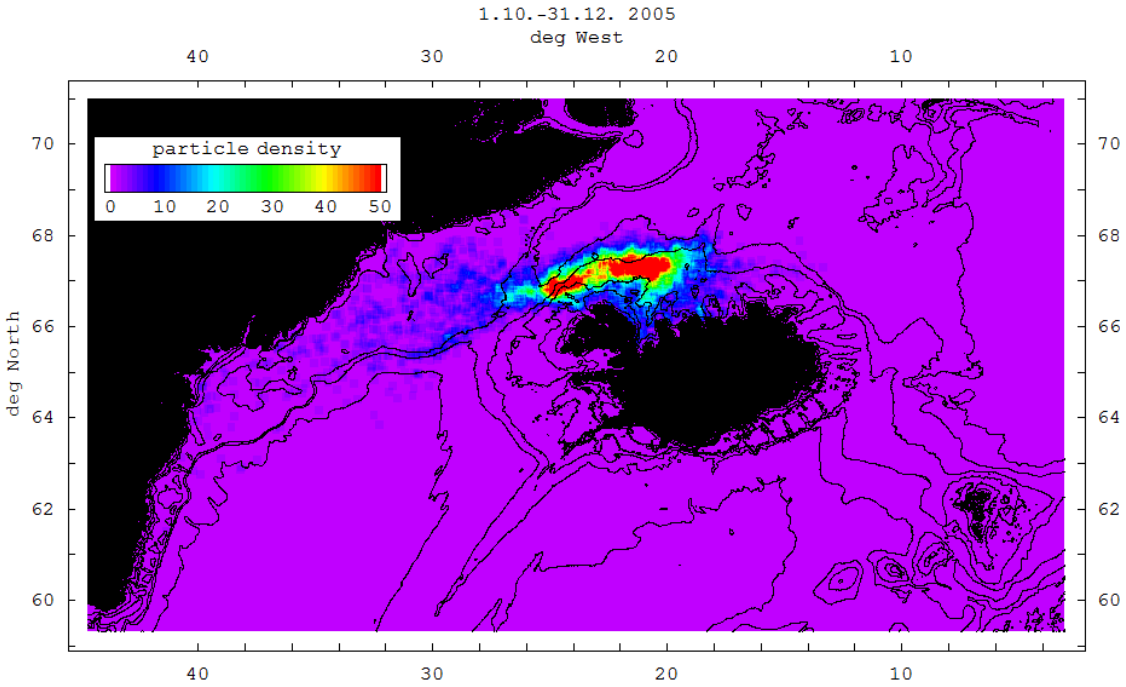

Fig. A1.7: Particle density at the end of the autumn 2005 simulation.

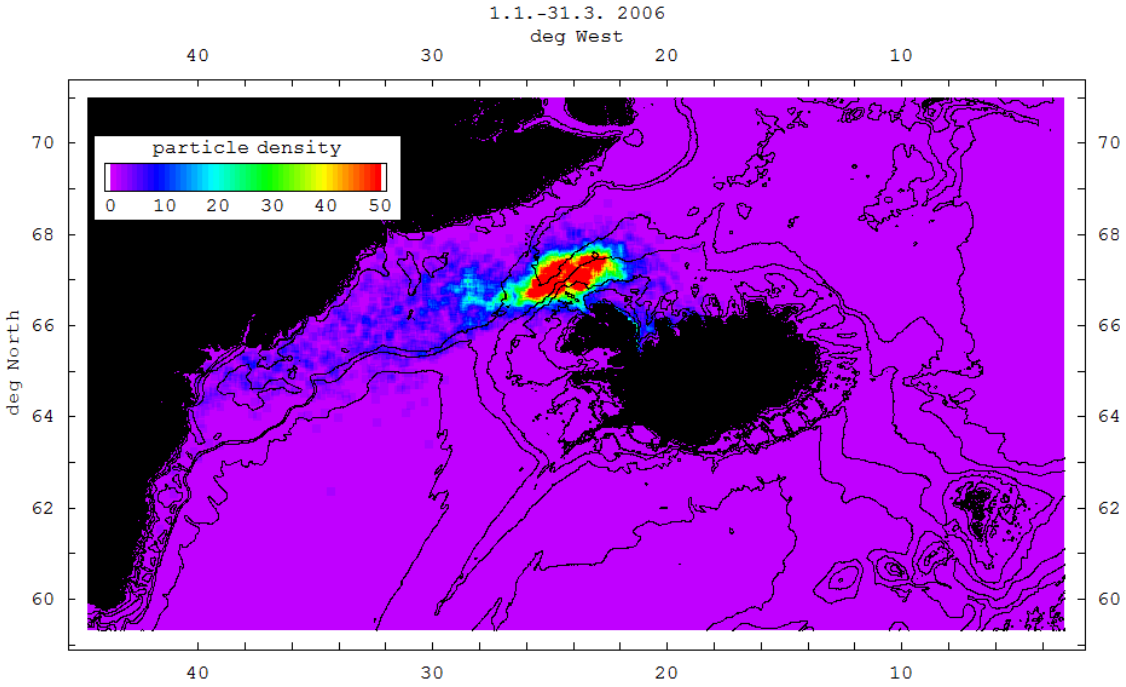

Fig. A1.8: Particle density at the end of the winter 2006 simulation.

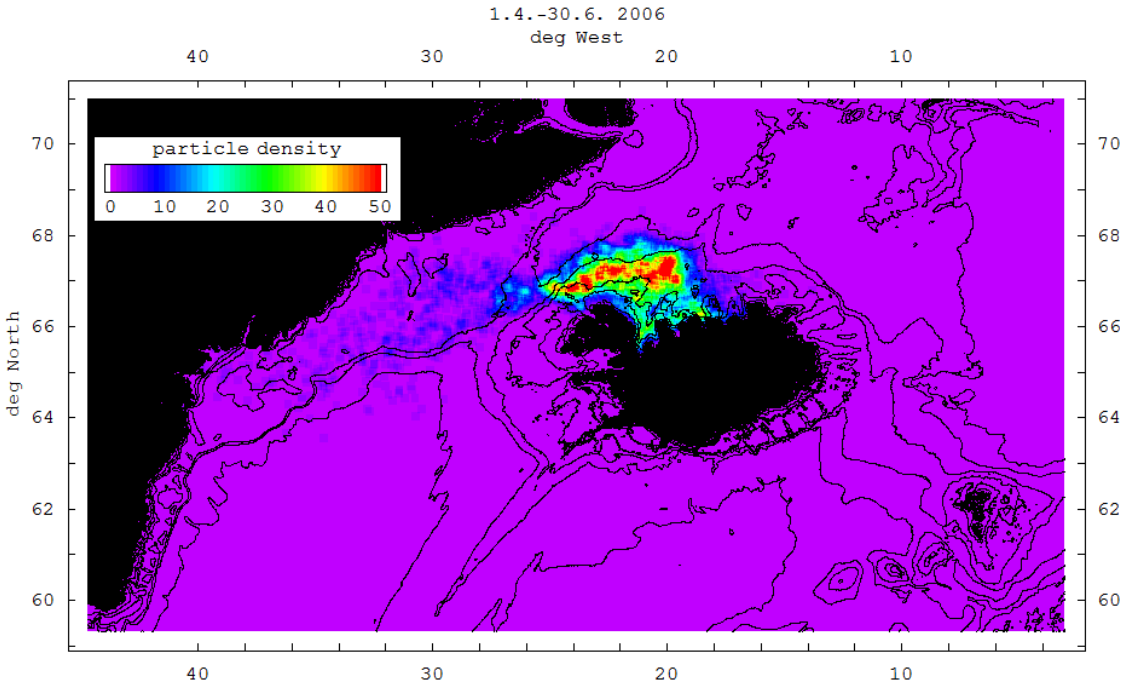

Fig. A1.9: Particle density at the end of the spring 2006 simulation.

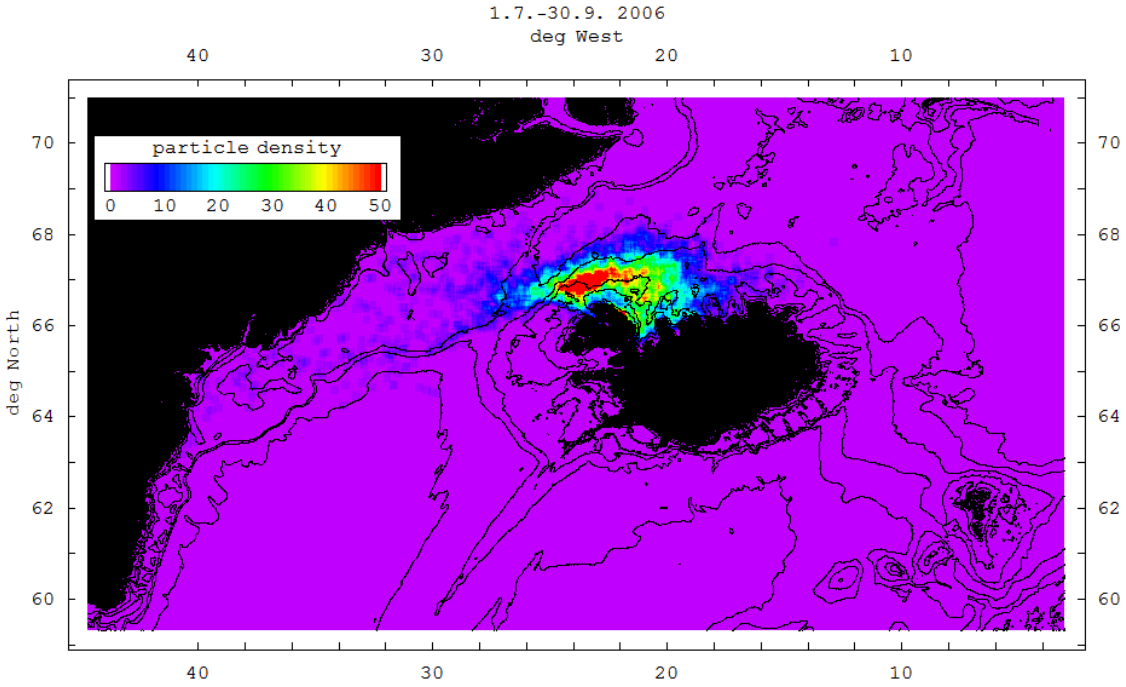

Fig. A1.10: Particle density at the end of the summer 2006 simulation.

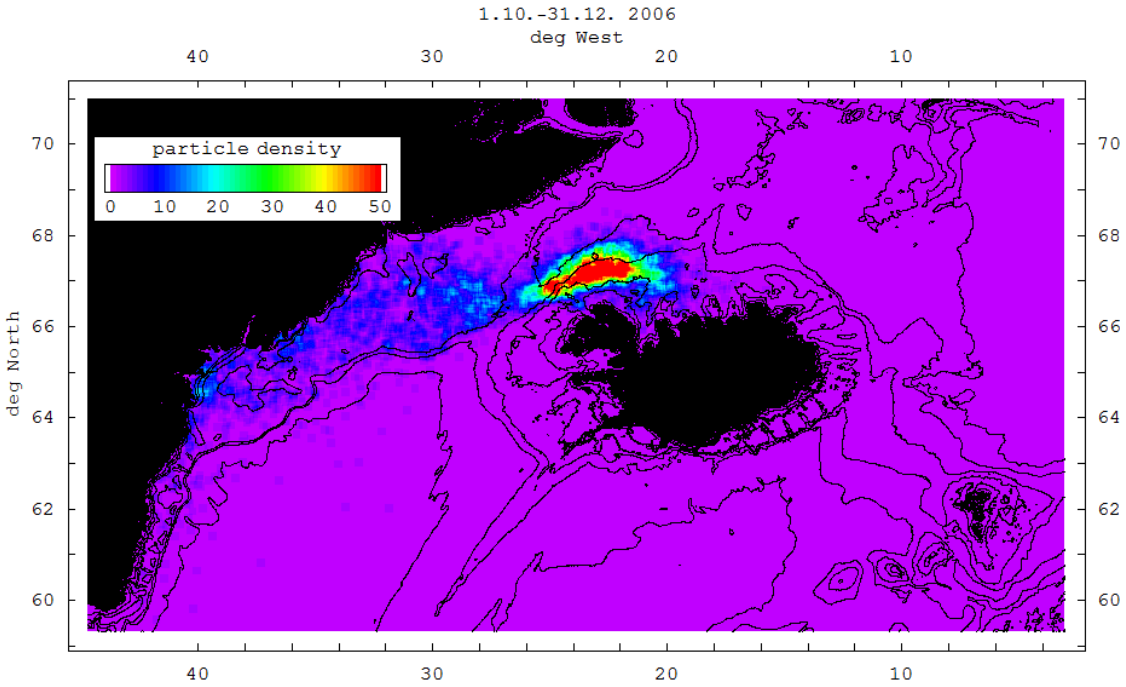

Fig. A1.11: Particle density at the end of the autumn 2006 simulation.

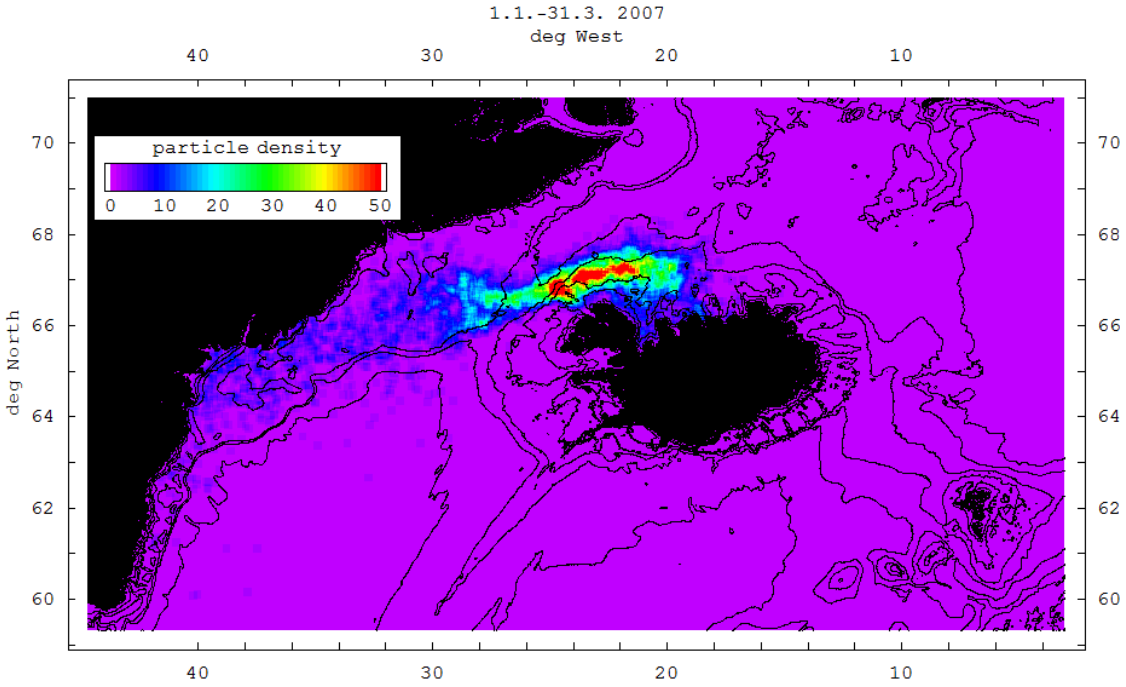

Fig. A1.12: Particle density at the end of the winter 2007 simulation.

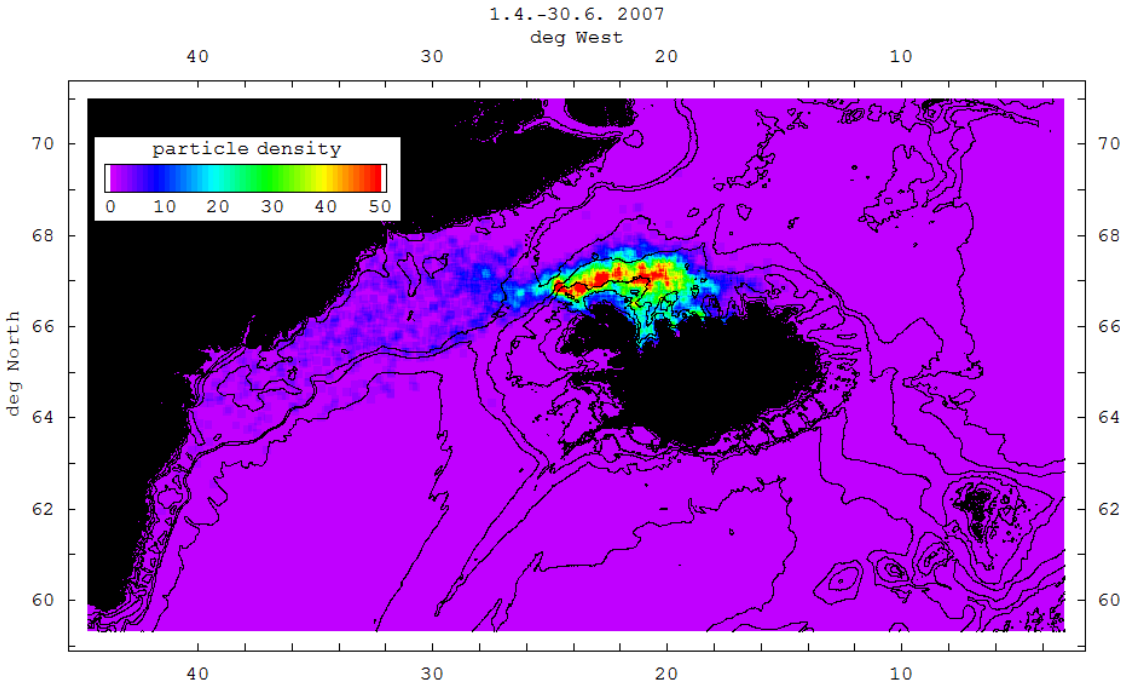

Fig. A1.13: Particle density at the end of the spring 2007 simulation.

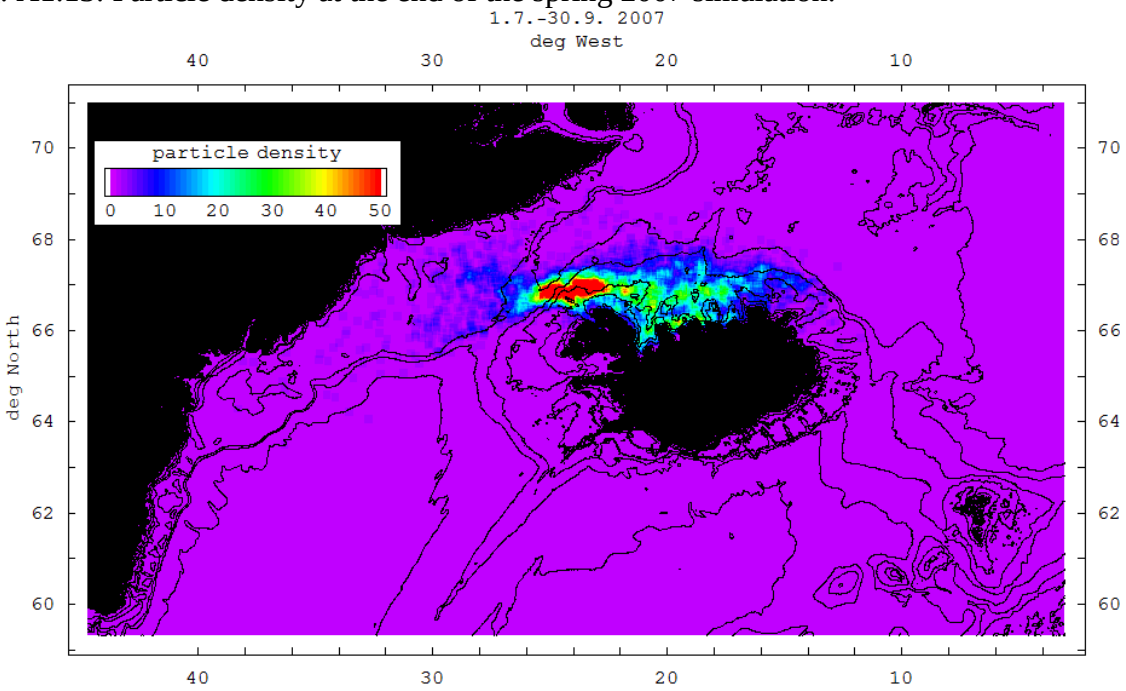

Fig. A1.14: Particle density at the end of the summer 2007 simulation.

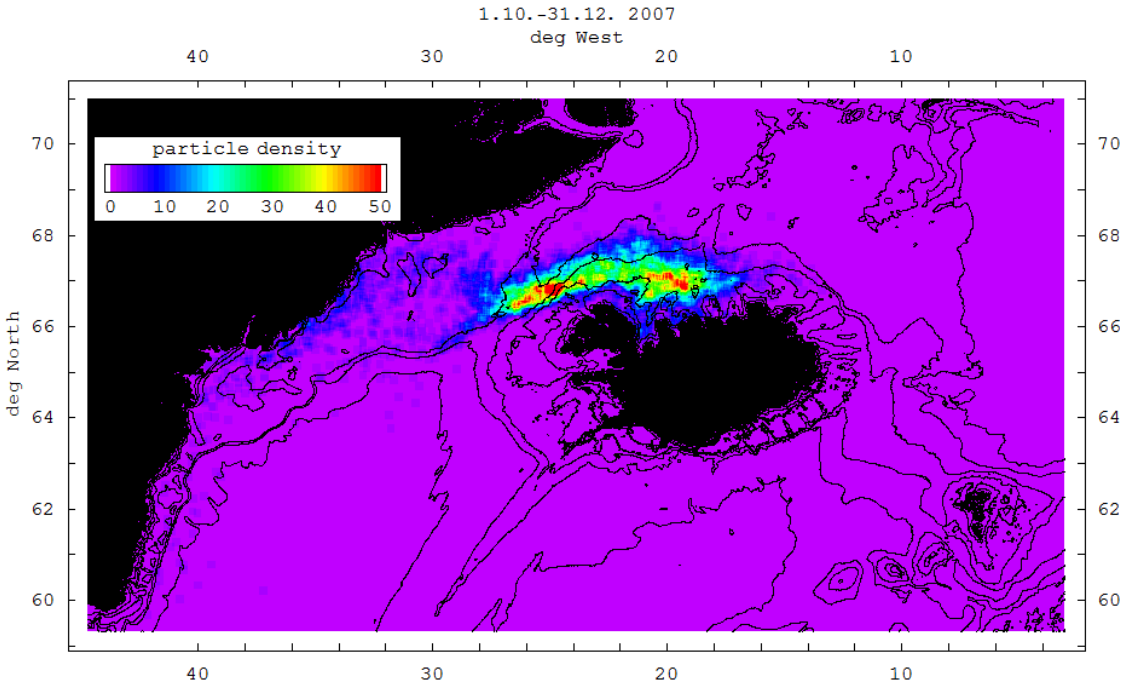

Fig. A1.15: Particle density at the end of the autumn 2007 simulation.

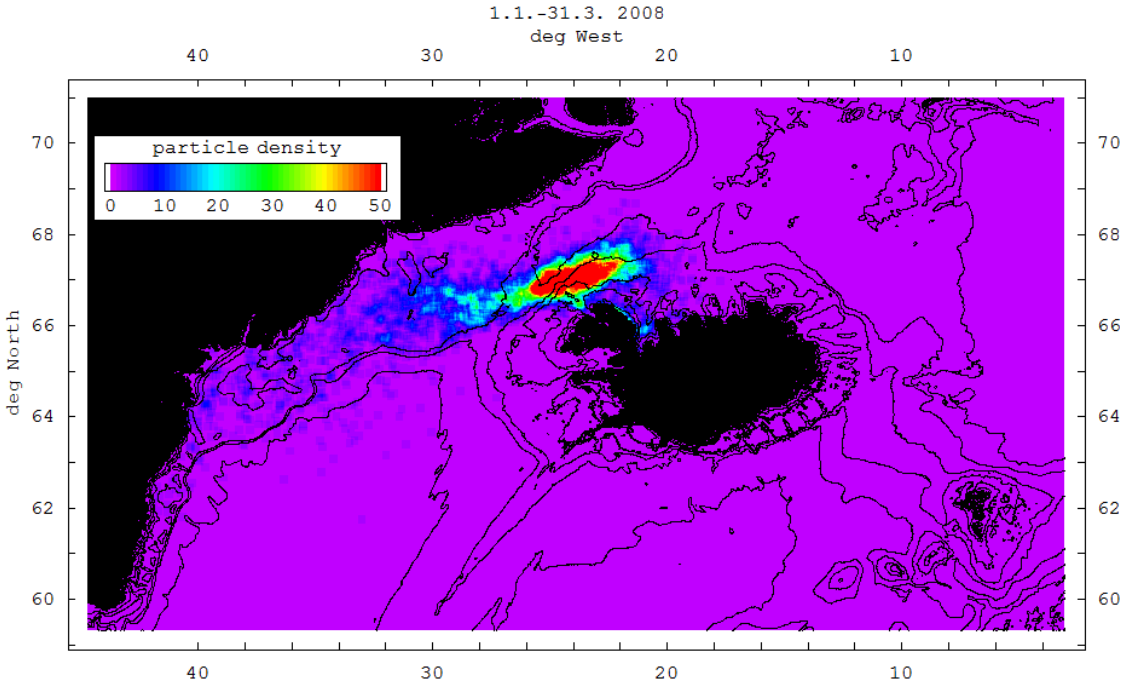

Fig. A1.16: Particle density at the end of the winter 2008 simulation.

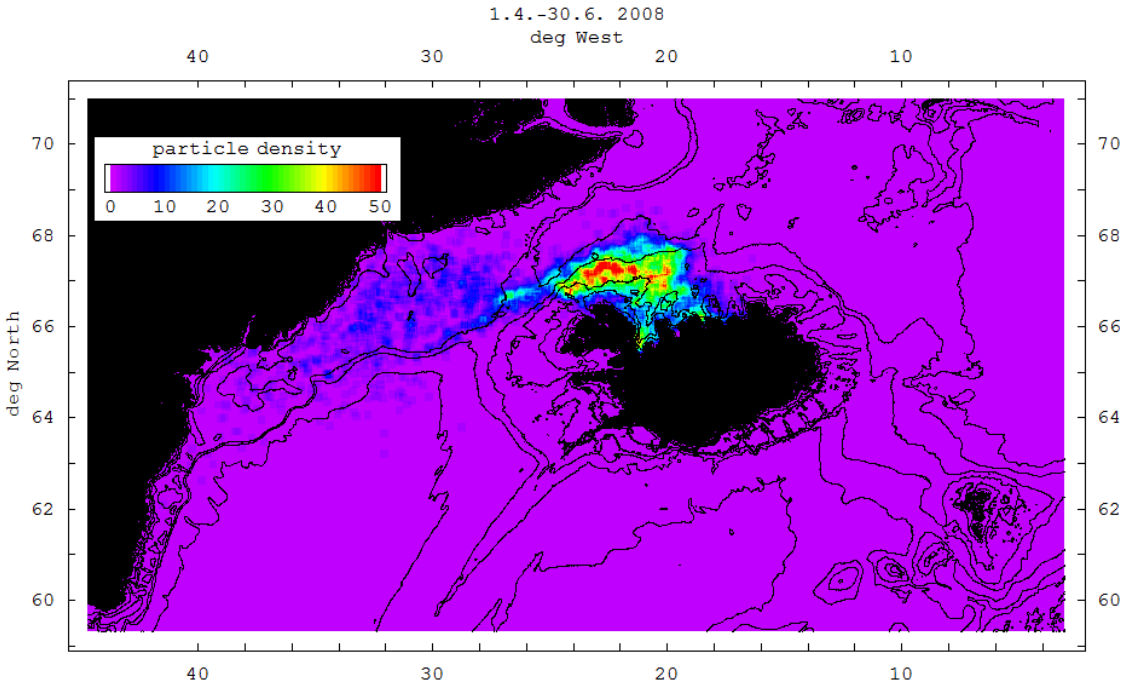

Fig. A1.17: Particle density at the end of the spring 2008 simulation.

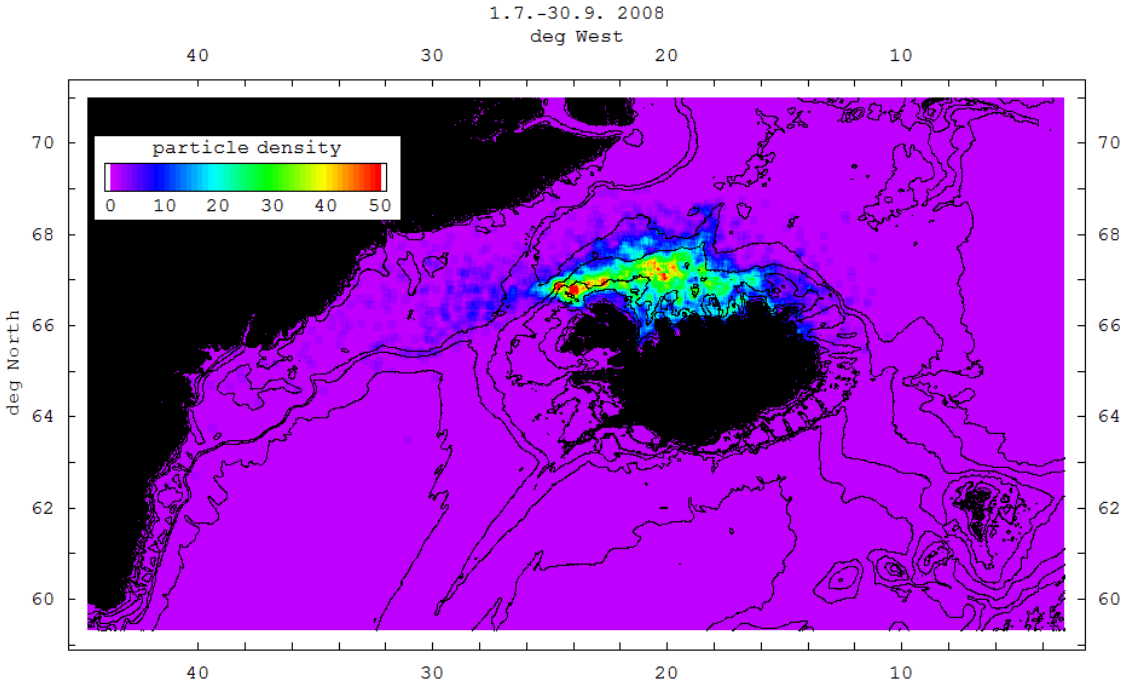

Fig. A1.18: Particle density at the end of the summer 2008 simulation.

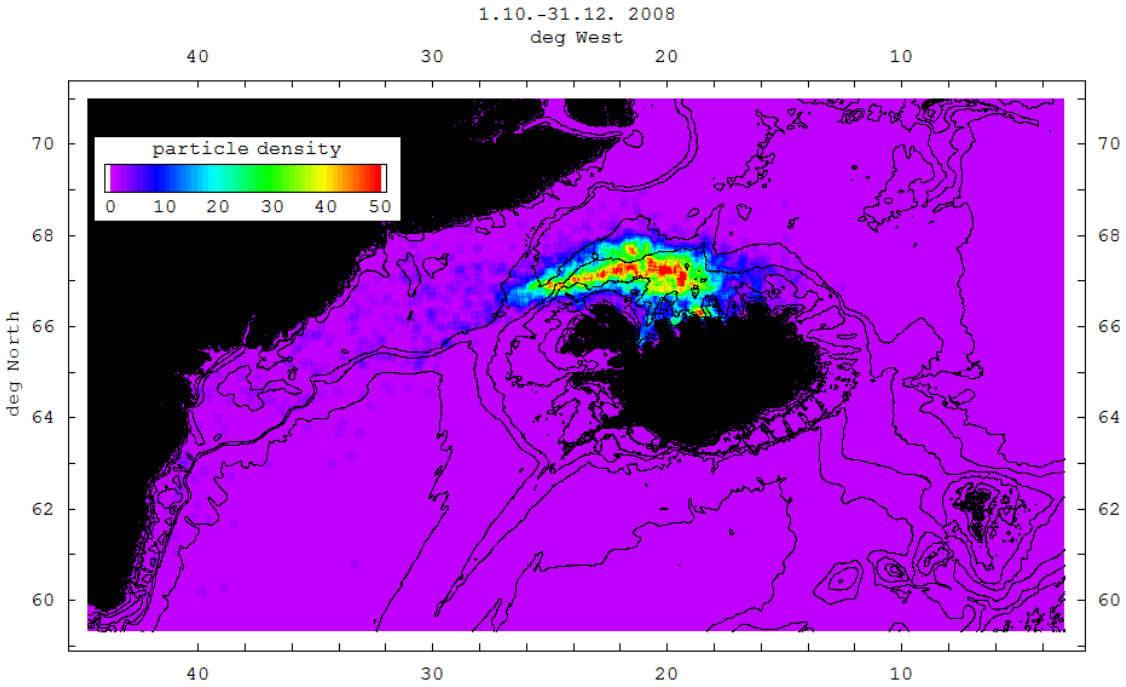

Fig. A1.19: Particle density at the end of the autumn 2008 simulation.

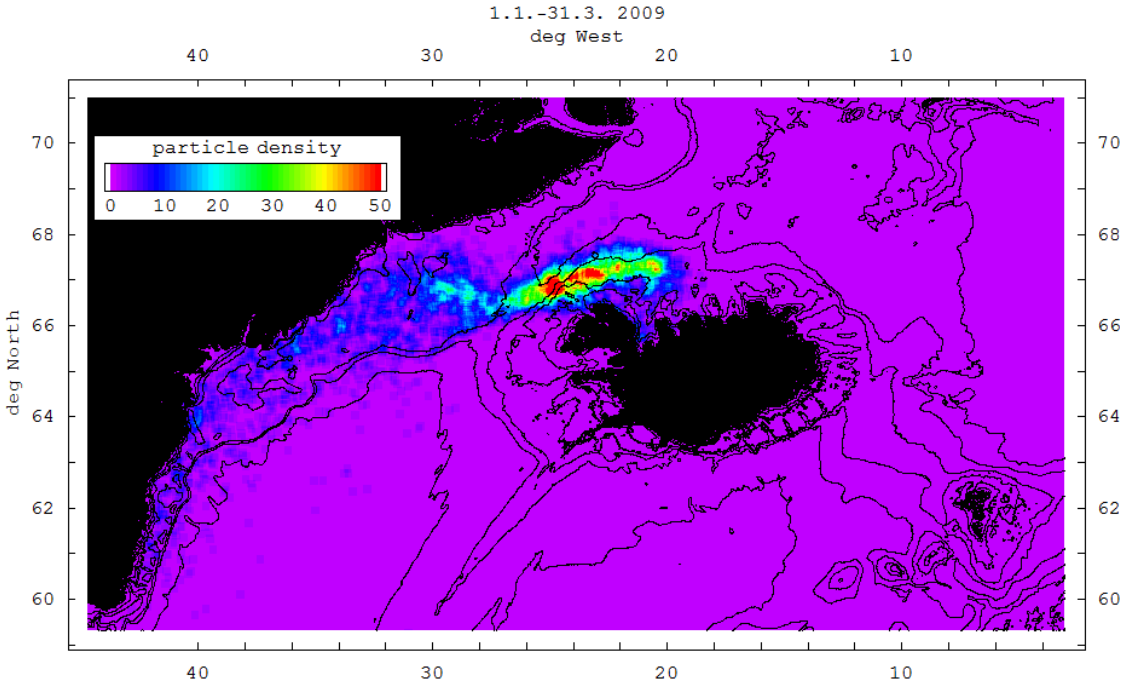

Fig. A1.20: Particle density at the end of the winter 2009 simulation.

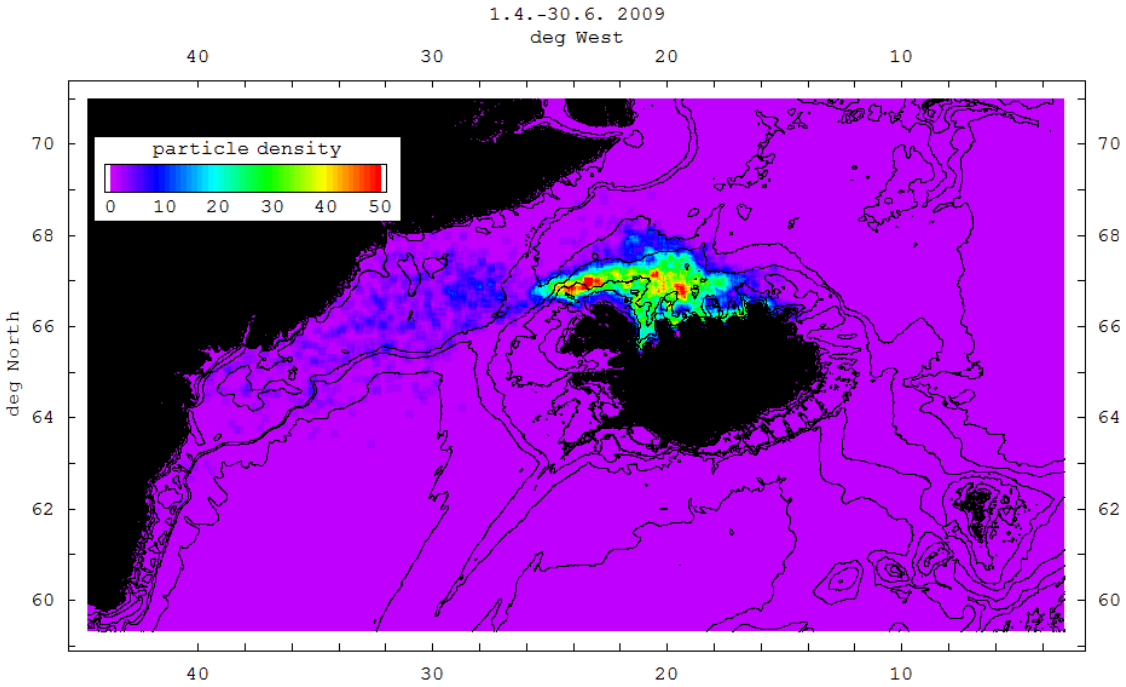

Fig. A1.21: Particle density at the end of the spring 2009 simulation.

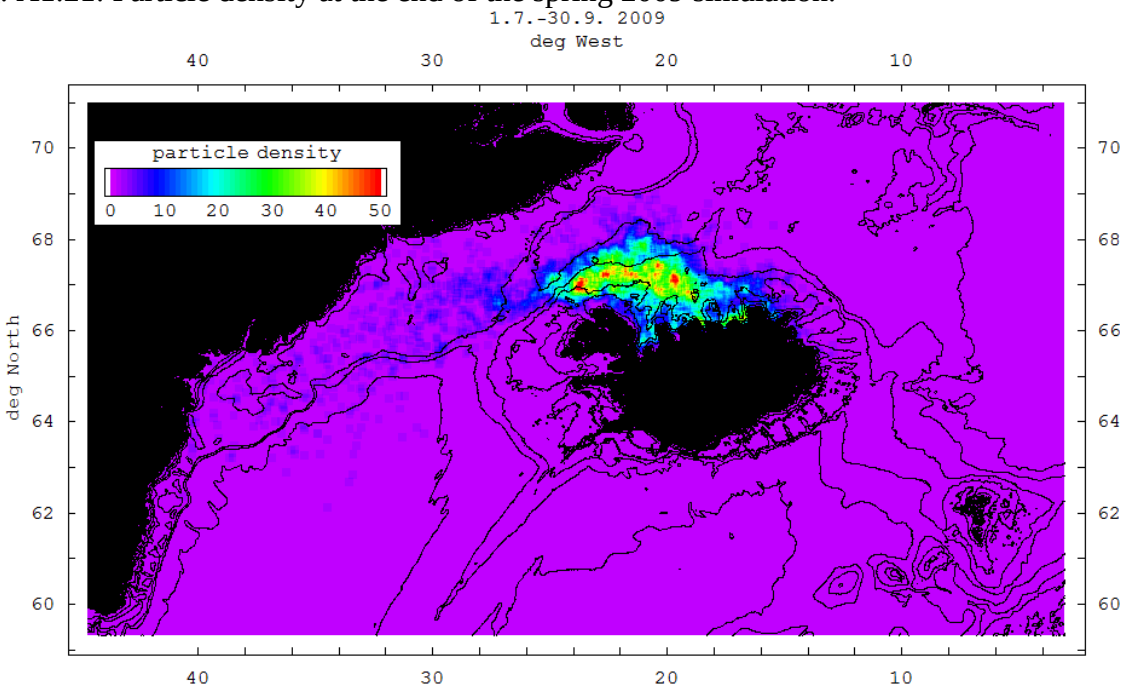

Fig. A1.22: Particle density at the end of the summer 2009 simulation.

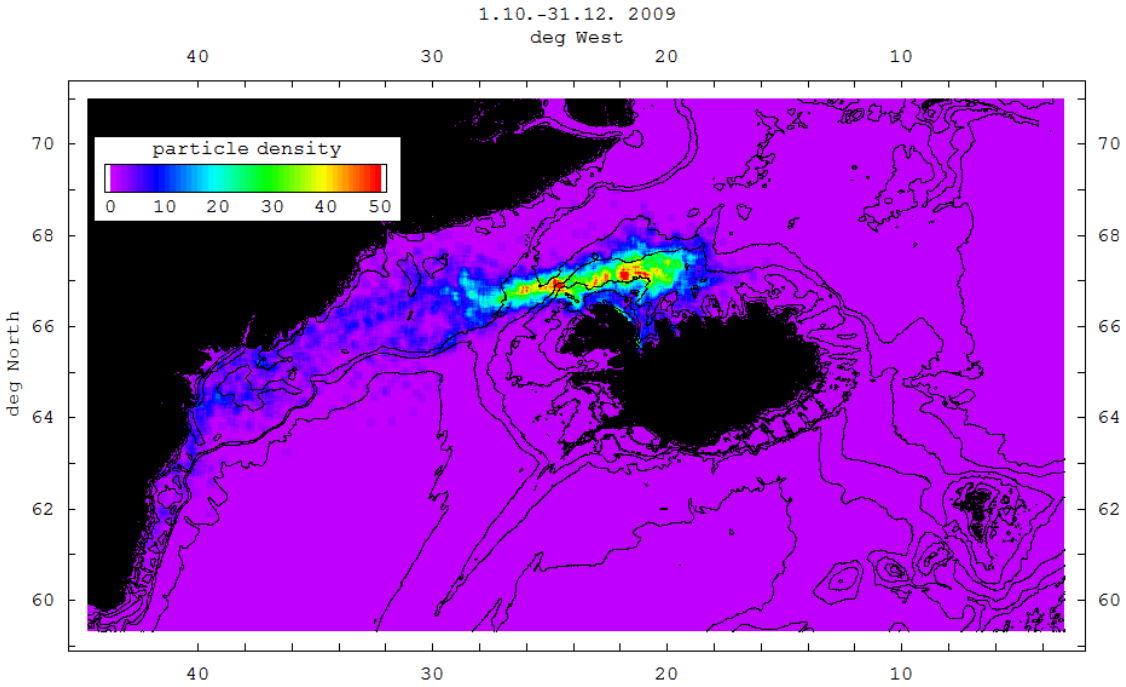

Fig. A1.23: Particle density at the end of the autumn 2009 simulation.

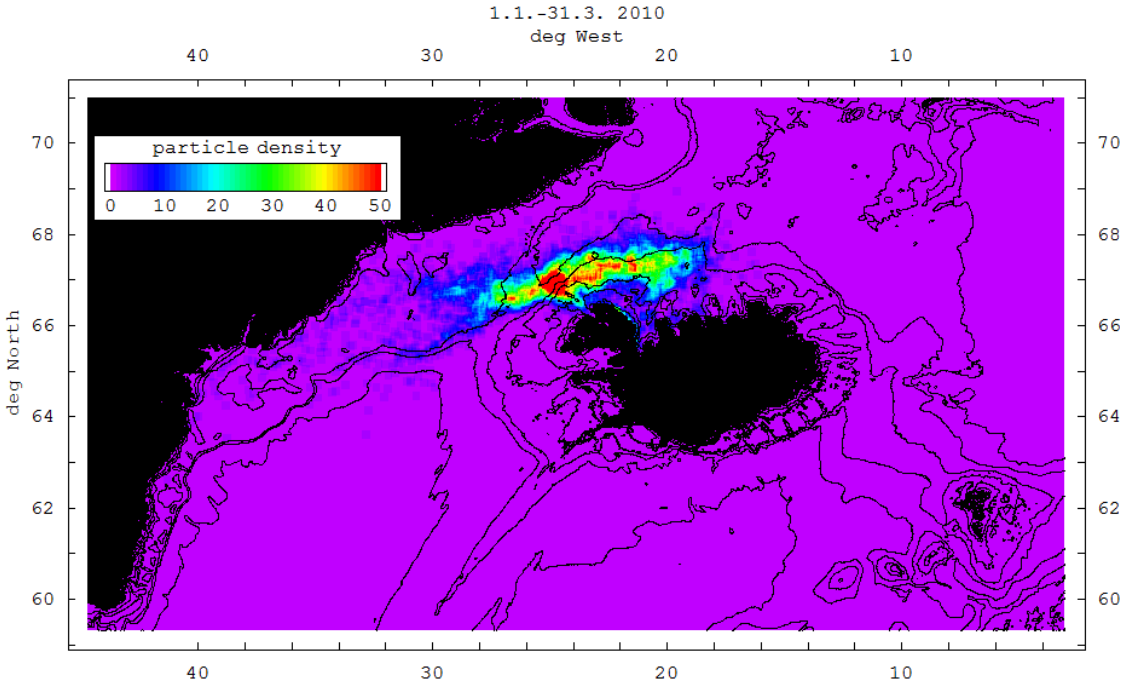

Fig. A1.24: Particle density at the end of the winter 2010 simulation.

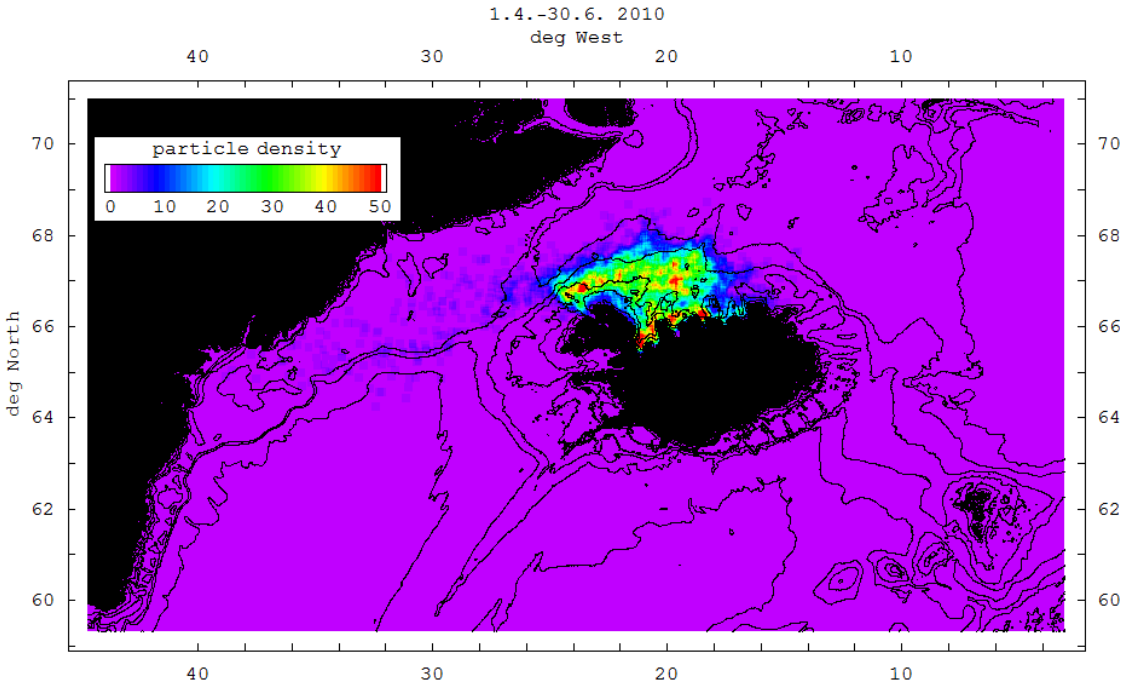

Fig. A1.25: Particle density at the end of the spring 2010 simulation.

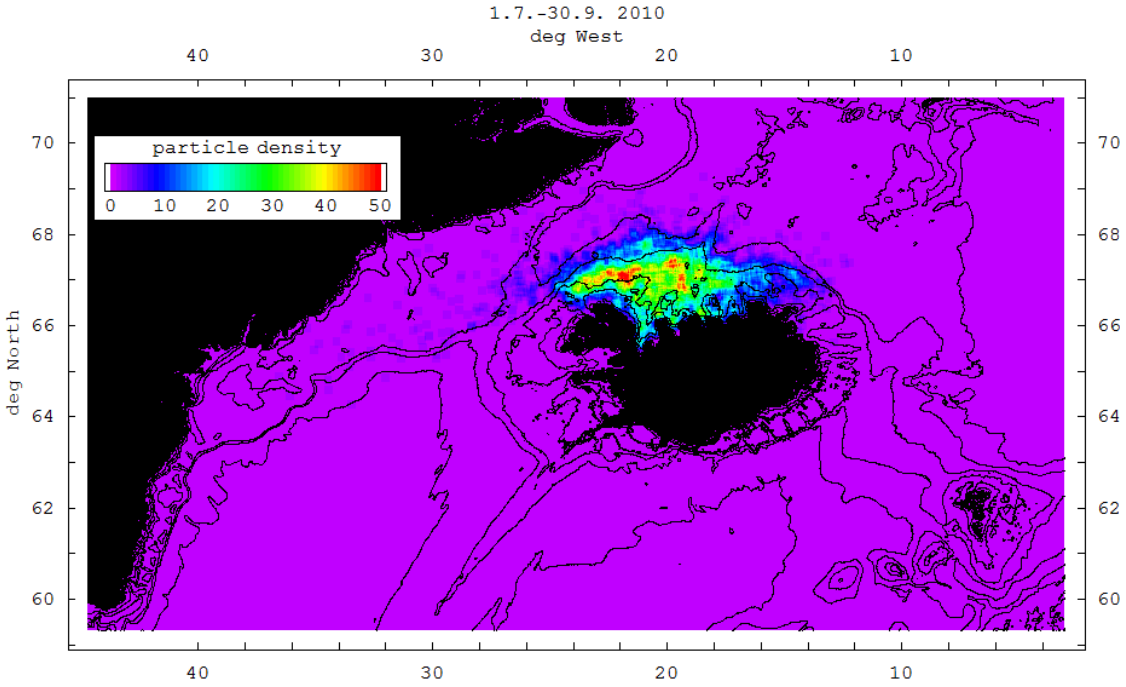

Fig. A1.26: Particle density at the end of the summer 2010 simulation.

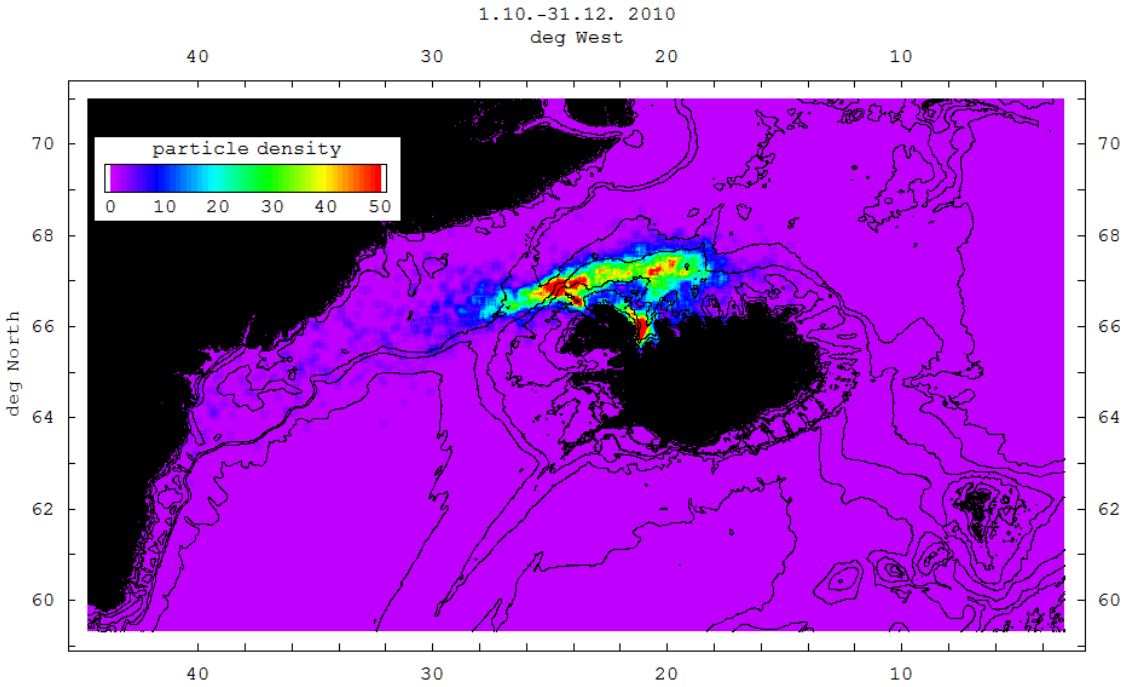

Fig. A1.27: Particle density at the end of the autumn 2010 simulation.

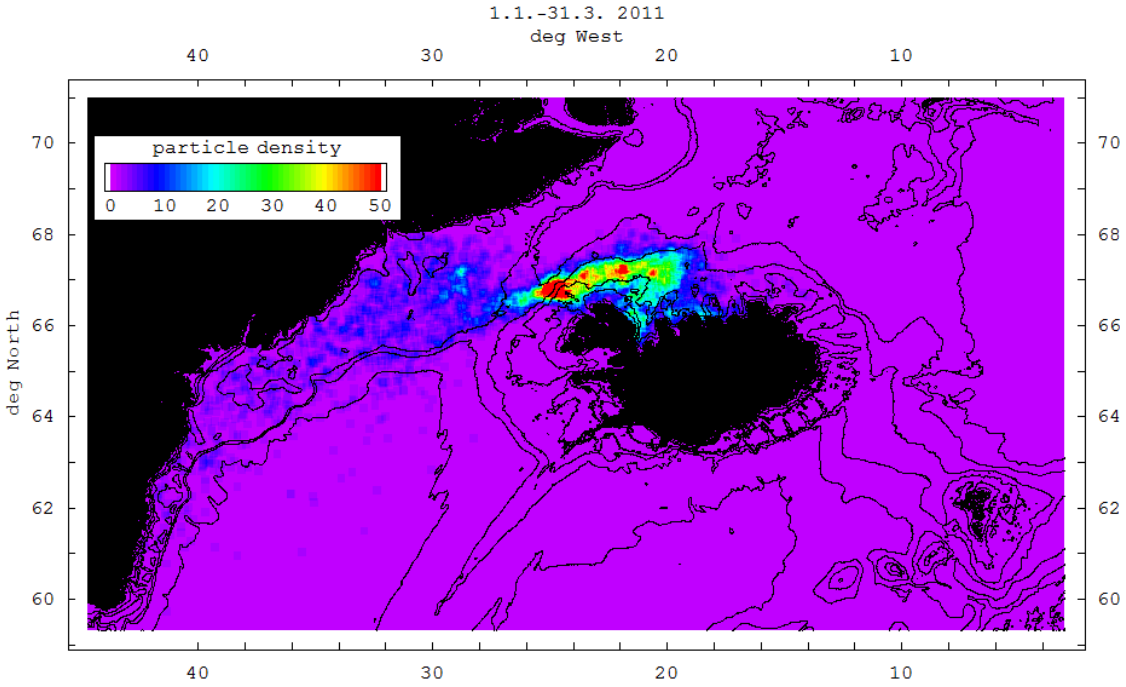

Fig. A1.28: Particle density at the end of the winter 2011 simulation.

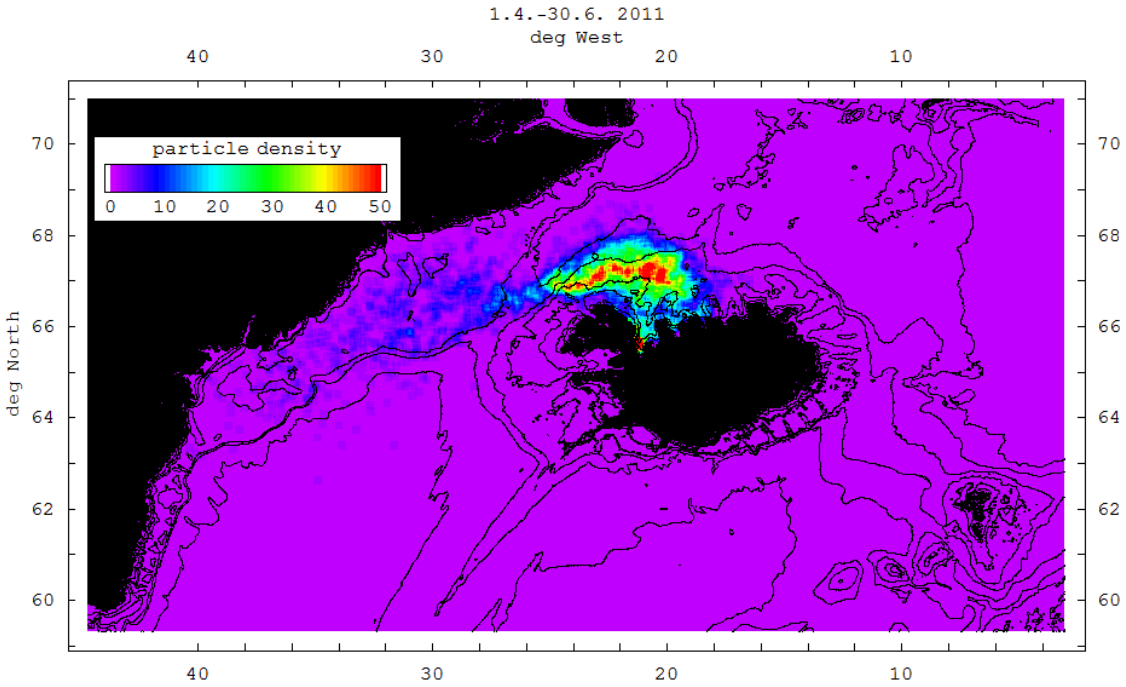

Fig. A1.29: Particle density at the end of the spring 2011 simulation.

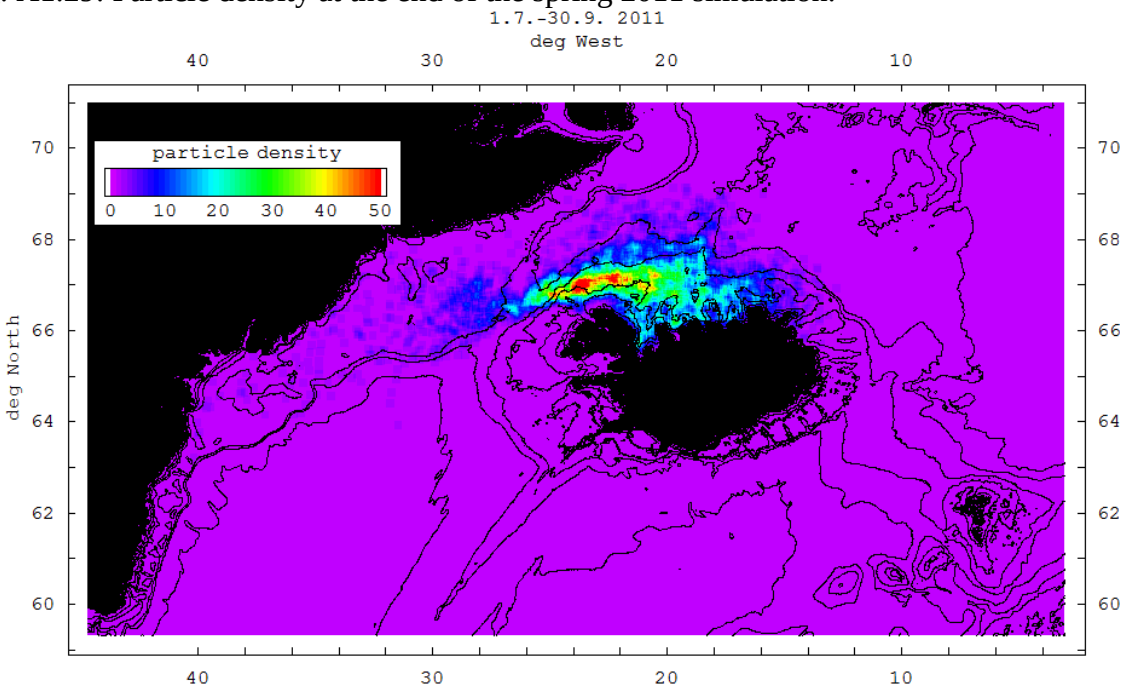

Fig. A1.30: Particle density at the end of the summer 2011 simulation.

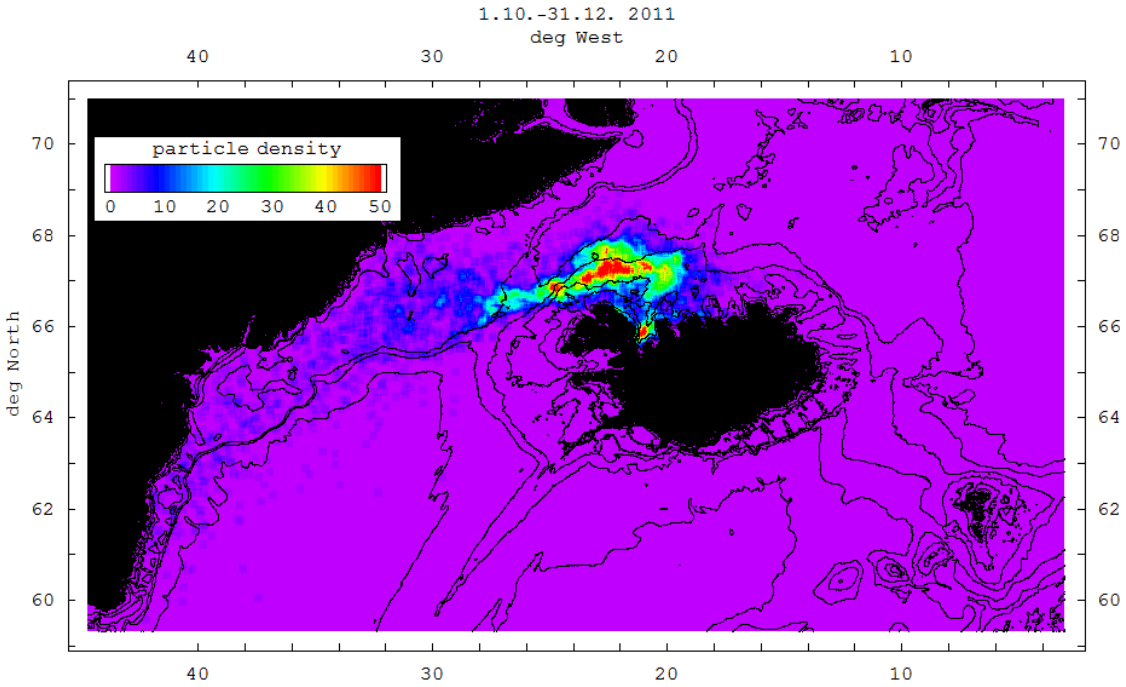

Fig. A1.31: Particle density at the end of the autumn 2011 simulation.

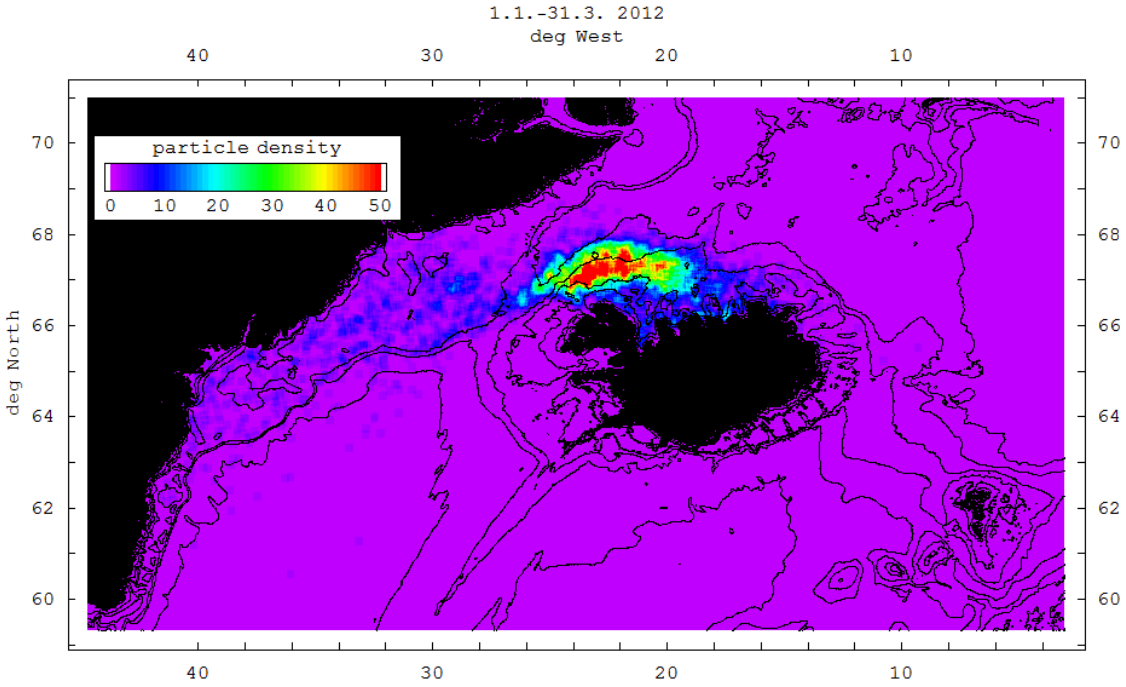

Fig. A1.32: Particle density at the end of the winter 2012 simulation.

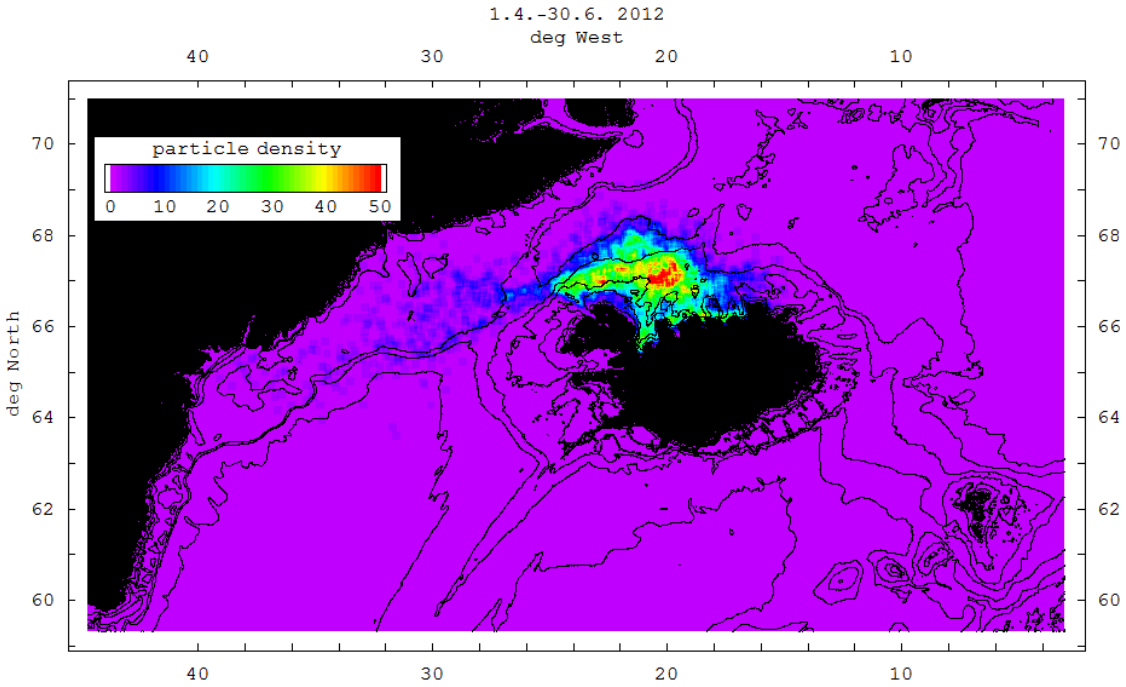

Fig. A1.33: Particle density at the end of the spring 2012 simulation.

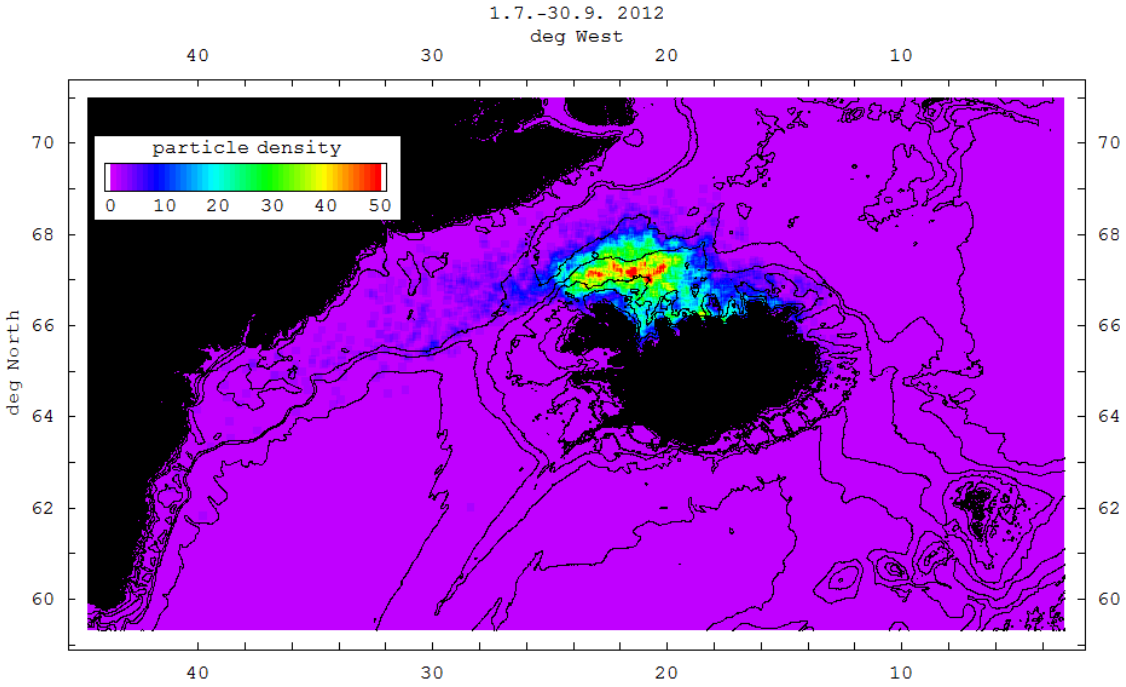

Fig. A1.34: Particle density at the end of the summer 2012 simulation.

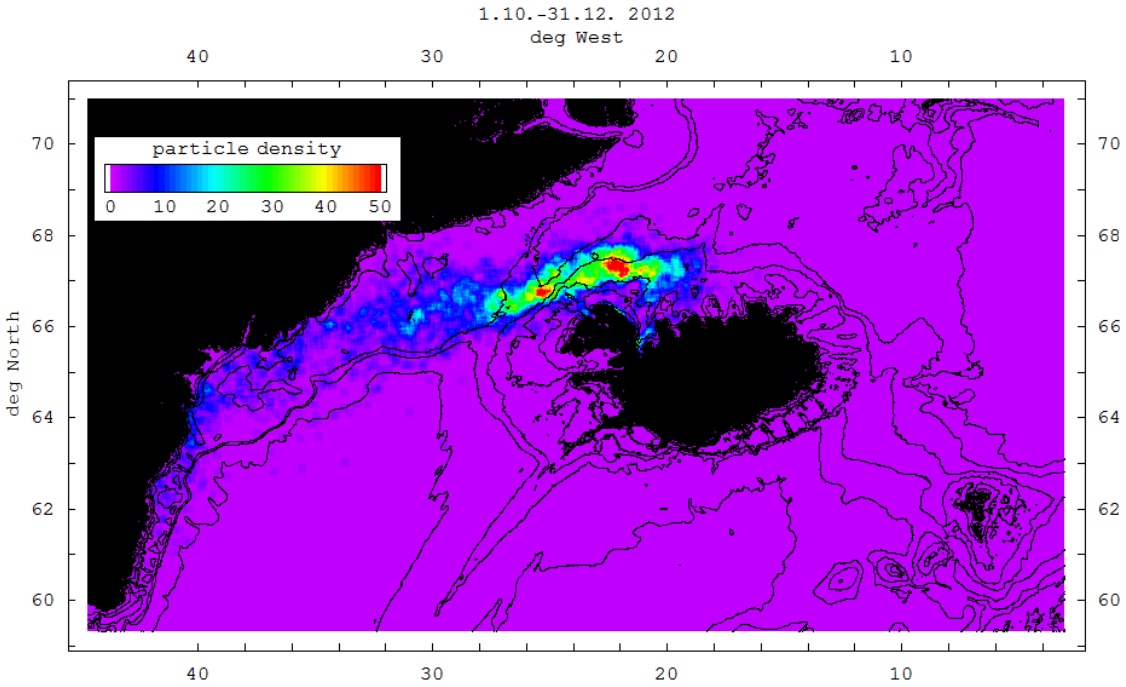

Fig. A1.35: Particle density at the end of the autumn 2012 simulation.

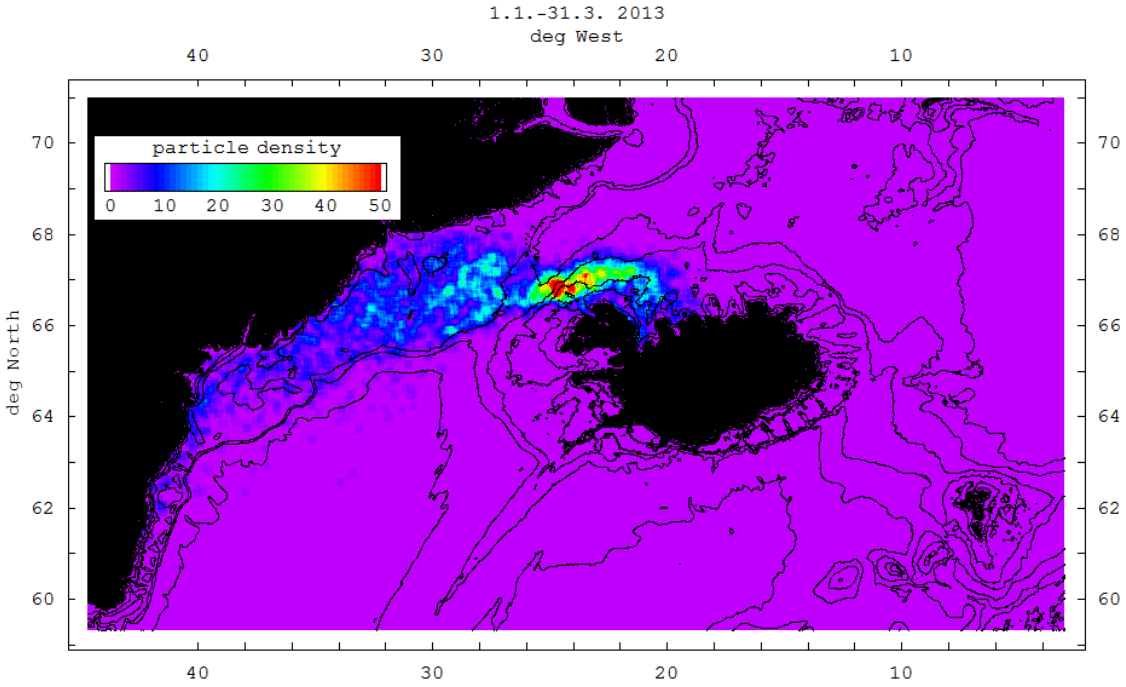

Fig. A1.36: Particle density at the end of the winter 2013 simulation.

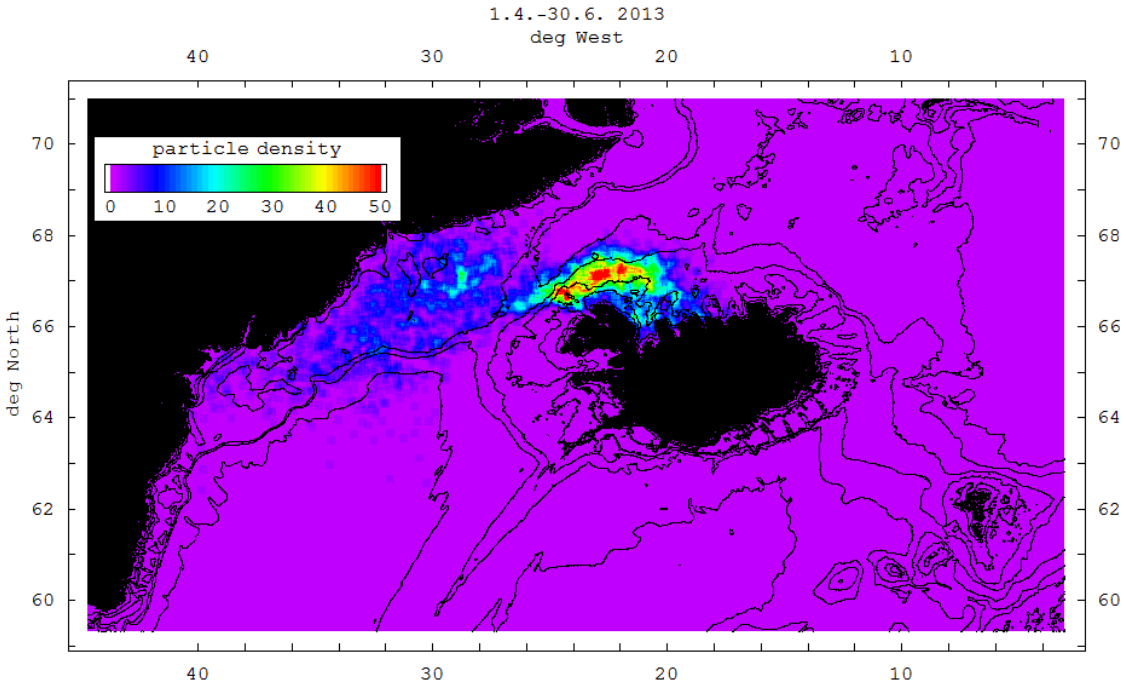

Fig. A1.37: Particle density at the end of the spring 2013 simulation.

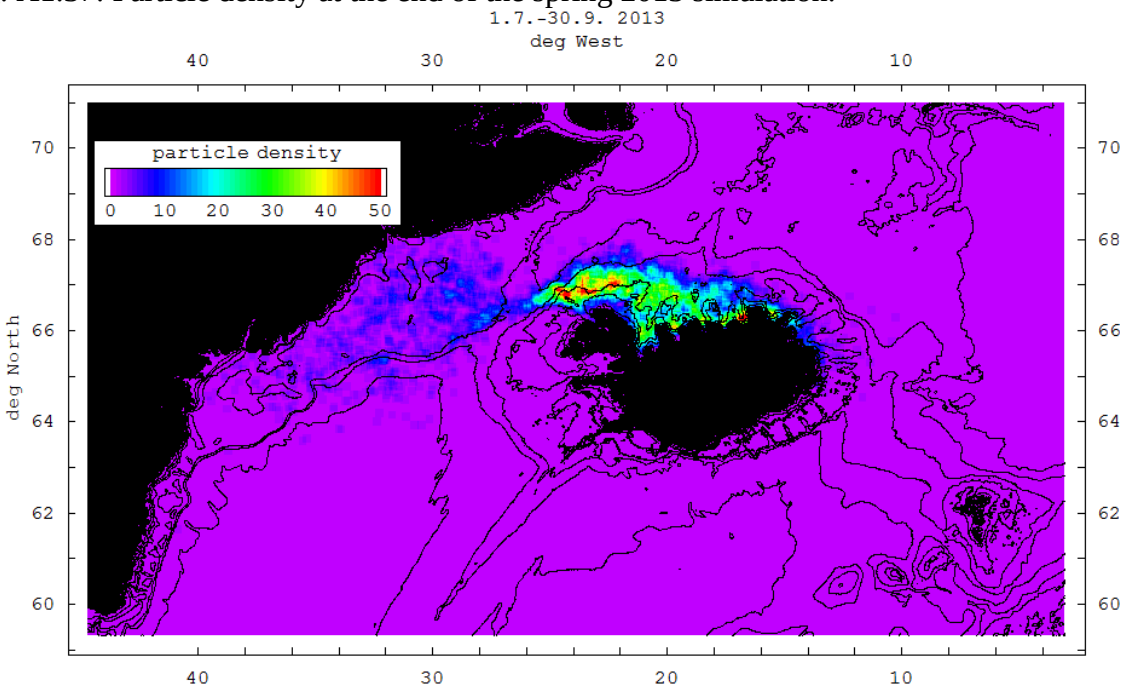

Fig. A1.38: Particle density at the end of the summer 2013 simulation.

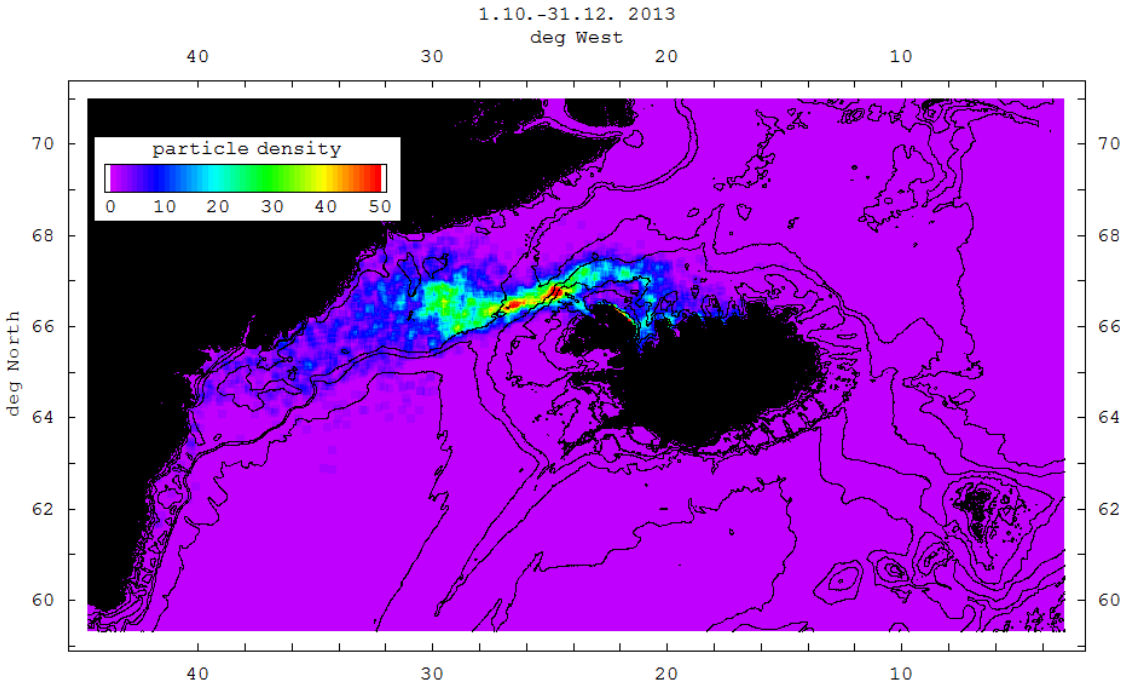

Fig. A1.39: Particle density at the end of the autumn 2013 simulation.

Appendix 2. NRPA box model description

The present model uses a modified approach for compartmental modelling (Iosjpe et al., 2002, 2009; Iosjpe, 2006) which allows the study of dispersion of radionuclides over time (non-instantaneous mixing in the oceanic space). The box structures for surface, mid-depth and deep water layers have been developed based on the description of polar, Atlantic and deep waters in the Arctic Ocean and the Northern Seas and site-specific information for the boxes generated from the 3D hydrodynamic model NAOSIM (Karcher and Harms, 2000). Surface structure is presented in Fig. A2.1.

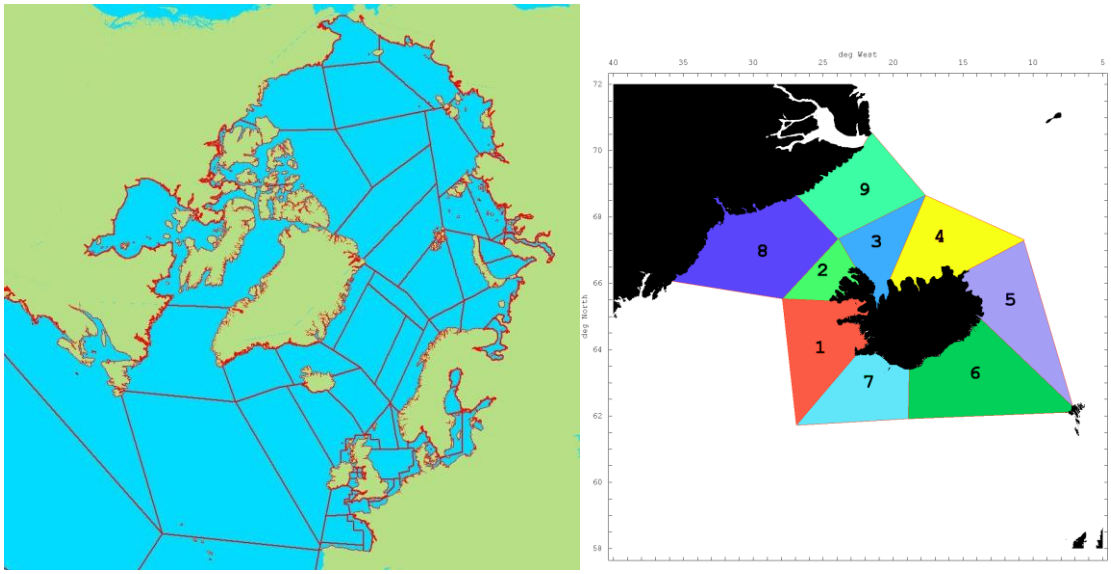

Figure A2.1. The structure of the surface water boxes for the NRPA box model and for the regional model for the Iceland coastal waters (COSEMA model).

The box model includes the processes of advection of radioactivity between compartments, sedimentation, diffusion of radioactivity through pore water in sediments, particle mixing, pore water mixing and a burial process of radioactivity in deep sediment layers. Radioactive decay is calculated for all compartments. Accumulation of contamination by biota is further calculated from radionuclide concentrations in filtered seawater in different water regions. Doses to humans are calculated on the basis from given seafood consumptions, based on available data for seafood catches and assumptions about human diet in the respective areas. Dose rates to biota are developed on the basis of calculated radionuclide concentrations in marine organisms, water and sediment, using dose conversion factors. Its structure is presented in Fig. A2.2.

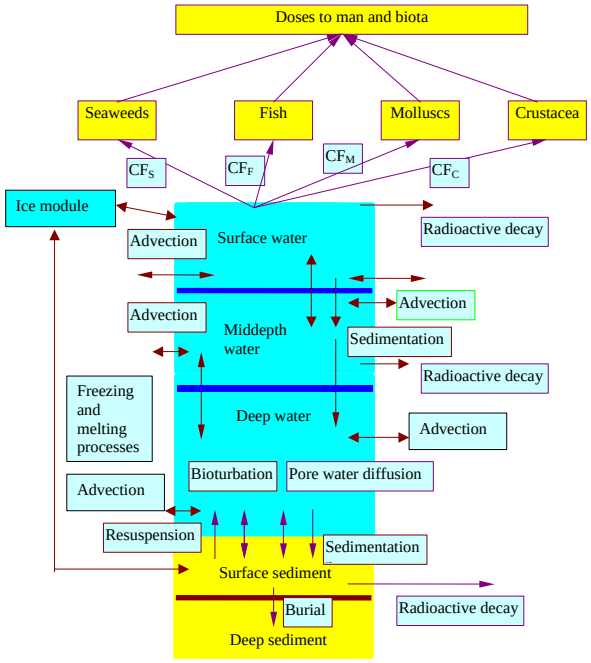

Figure A2.2. A schematic structure of the processes involved in modelling.

The equations of the transfer of radionuclides between the boxes are of the form:

$$\frac{dA_i}{dt} = \sum_{j=1}^{n} k_{ji} A_j \gamma[t \geq (T_j + w_{ji})] - \sum_{j=1}^{n} k_{ij} A_i \gamma[t \geq (T_i + w_{ij})] - k_i A_i \gamma(t \geq T_i) + Q_i, \; t \geq T_i$$

$$A_i = 0, t < T_i \qquad \text{(A1)}$$

where $k_{ii}=0$ for all i, A_i and A_j are activities (Bq) at time t in boxes i and j; k_{ij} and k_{ji} are rates of transfer (y^{-1}) between boxes i and j; k_i is an effective rate of transfer of activity (y^{-1}) from box *i* taking into account loss of material from the compartment without transfer to another, for example radioactive decay; Q_i is a source of input into box i (Bq y^{-1}); n is the number of boxes in the system, T_i is the time of availability for box i (the first times when box i is open for dispersion of radionuclides) and γ is an unit function:

$$\gamma(t \geq T_i) = \begin{cases} 1, t \geq T_i \\ 0, t < T_i \end{cases}.$$

The times of availability T_i

$$T_i = \min_{\mu_m (v_0, v_i) \in M_i} \sum_{j,k} w_{jk}$$

are calculated as a minimized sum of the weights for all paths $\mu_m(v_0,...,v_i)$ from the initial box (v_0) with discharge of radionuclides to the box i on the oriented graph G=(V, E) with a set V of nodes v_j correspondent to boxes and a set E of arcs e_{jk} correspondent to the transfer possibility between the boxes j and k (graph elements as well as available paths are illustrated by Figure A2.3). Every arc e_{jk} has a weight w_{jk} which is defined as the time required before the transfer of radionuclides from box j to box k can begin (without any way through other boxes). Weight, w_{jk}, is considered as a discrete function F of the water fluxes f_{jk}, f_{kj} between boxes j and k, geographical information g_{jk} and expert evaluation X_{jk}. M_i is a set of feasible paths from the initial box (v_0) to the box i (v_i).

It is interesting to note that traditional box modelling is a particular case of the present approach when all times of availability in (A1) are zero: $\{T_i\} = 0, i = 1,\ldots, n.$

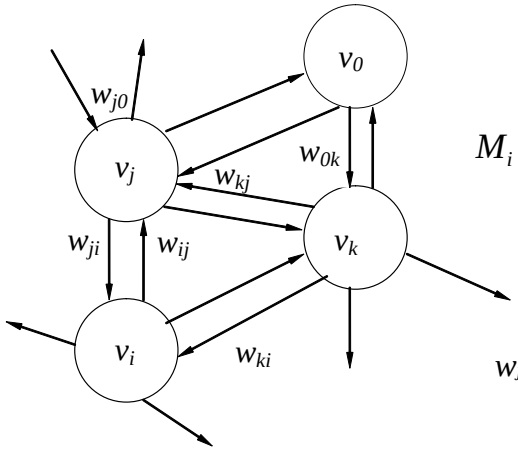

$$M_i = \begin{cases} \mu_1(v_0, v_j, v_i) \\ \mu_2(v_0, v_k, v_i) \\ \mu_3(v_0, v_j, v_k, v_i) \\ \mu_4(v_0, v_k, v_j, v_i) \end{cases}$$

$$w_{jk} = F(f_{jk}, f_{kj}, g_{jk}, X_{jk})$$

Figure A2.3. Graph elements.

Expressions for the transfer rates of radioactivity between the bottom water and sediment compartments will be useful in the present analysis (the transfer rates are shown in Figure A2.4):

$$k_{WS} = \frac{SR \cdot k_d}{d \cdot (1 + k_d \cdot SSL)} + \frac{D}{d \cdot h_S (1 + k_d \cdot SSL)} + \frac{R_T \cdot \omega \cdot h_S}{d \cdot (1 + k_d \cdot SSL)} + \frac{R_W \cdot \rho \cdot k_d \cdot (1-\omega)}{d \cdot (1 + k_d \cdot SSL)}$$

$$k_{SW} = \frac{D}{h_S^2 \cdot [\omega + k_d \cdot \rho \cdot (1-\omega)]} + \frac{R_T \cdot \omega}{\omega + k_d \cdot \rho \cdot (1-\omega)} + \frac{R_W \cdot \rho \cdot k_d \cdot (1-\omega)}{h_S \cdot [\omega + k_d \cdot \rho \cdot (1-\omega)]}$$

$$k_{SM} = \frac{D \cdot \omega}{h_S^2 \cdot [\omega + k_d \cdot \rho \cdot (1-\omega)]} + \frac{k_d \cdot SR}{h_S \cdot [\omega + k_d \cdot \rho \cdot (1-\omega)]}$$

$$k_{MS} = \frac{D \cdot \omega}{h_S \cdot h_{SM} \cdot [\omega + k_d \cdot \rho \cdot (1-\omega)]}$$

$$k_{MD} = \frac{k_d \cdot SR}{h_{SM} \cdot [\omega + k_d \cdot \rho \cdot (1-\omega)]}.$$

Here k_{WS} is composed of expressions describing the transfer of activity by sedimentation, molecular diffusion, pore water mixing and particle mixing, respectively. Similarly, k_{SW} is composed of expressions describing the transfer of radioactivity by molecular diffusion, pore water mixing and particle mixing. k_{SM} is composed of expressions describing the transfer of radioactivity by sedimentation and molecular diffusion. k_{MS} corresponds to the transfer by molecular diffusion. Finally, k_{MD} corresponds to the transfer of radioactivity by sedimentation. R_W (m y^{-1}) is the sediment reworking rate; R_T (y^{-1}) is the pore-water turnover rate; k_d (m^3 t^{-1}) is the sediment distribution coefficient; *SSL* (t m^{-3}) is the suspended sediment load in the water column; *SR* (t m^{-2} y^{-1}) is the sedimentation rate; *D* (m^2 y^{-1}) is the molecular diffusion coefficient, h_S (m) and h_{SM} (m) are the surface and middle sediment thickness respectively; ω is the porosity of the bottom sediment; ρ (t m^{-3}) is the density of the sediment material and *d* is the depth of the water column.

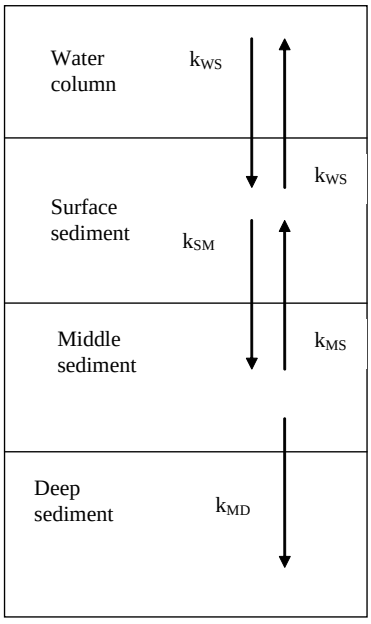

Figure A2.4. Generic vertical structure of the water-sediment compartments.

References

Iosjpe M., 2006. Environmental Modelling: Modified Approach for Compartmental Models. In: Radionuclides in the Environment. Edd. P.P. Povinec, J.A. Sanchez-Cabeza. Radioactivity in the Environment, vol. 8, Series Editor: M.S. Baxter, 2006, 463-476.

Iosjpe M., Brown J. & Strand P. (2002). Modified Approach for Box Modelling of Radiological Consequences from Releases into Marine Environment, Journal of Environmental Radioactivity, Vol. 60, No 1-2, 91-103.

Iosjpe M., M. Karcher, J. Gwynn, I. Harms, R. Gerdes and F. Kauker (2009). Improvement of the dose assessment tools on the basis of dispersion of the ^{99}Tc in the Nordic Seas and the Arctic Ocean. *Radioprotection*, vol. **44**, n^{o} 5, 531-536.

Karcher M.J. and Harms I.H., 2000. Estimation of water and ice fluxes in the Arctic for an improved box structure of the NRPA box model. In: Iosjpe M. (Ed.): Transport and fate of contaminants in the Northern Seas, NRPA, 2000.

The biological half-life of Cs-137 in primary producers and the effective half-lives of Cs-137 in surface water in different basins of the Baltic Sea is shown below.

Appendix 3. The biological half-life for species and effective half-life of Cs-137 for the Baltic Sea

The biological half-life of Cs-137 in primary producers and the effective half-lives of Cs-137 in surface water in different basins of the Baltic Sea are shown below.

Table A3.1. Effective half-lives of Cs-137 in surface water. Data is taken from HELCOM MORS Baltic Sea Environment Proceedings No. 135.

Baltic Sea Region	**1986-1988**	**1993-2006**	**1993-2010**
Bothnian Bay	-	10	9
Bothnian Sea	2.5	9	9
Gulf of Finland	0.8	13	11
Baltic Sea proper	-	15	11

Table A3.2. The biological half-life of Cs-137 in primary producers. Data taken from U.S. Environmental Protection Agency 1986 520/1-85-015. (algae)

Organism	**Biological half-life in days**
Ulva lactuca	5
Codium decorticatum	15
Fucus vesiculosus	8
Porphyra umbilicalis	3
Chondrus crispus	2
Gracilaria foliifera	12
Agardhiella tenera	21
Halimeda incrassata	3

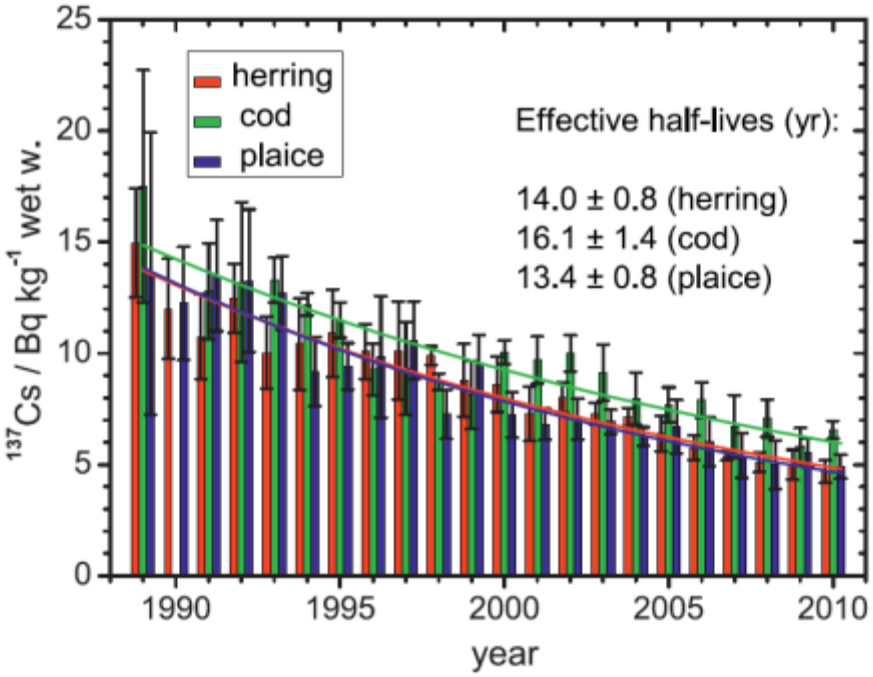

Figure A3.1. Effective half-lives for fish for the Poland coastal waters.

Fish consumption.

It is estimated that the fish consumption consist of 80% zooplankton, 10% benthic plants, 5% benthos and 5% grazing macrofauna (Kumblad et al., 2003).

References

Kumblad L., Gilek M., Næslund B., Kautsky U. (2003). An ecosystem model of the environmental transport and fate of carbon-14 in a bay of the Baltic Sea, Sweden, Ecological modelling 166 (3), 193-210, 2003.

Bibliographic Data Sheet **NKS-326**

Title	Effects of dynamic behaviour of Nordic marine environment to radioecological assessments
Author(s)	Halldórsson[1] Ó., Iosjpe[2] M., Isaksson[3] M., Joensen[4] H. P., Jonsson[1] G., Logemann[5] K., Roos[6] P., Suolanen[7] V., Thomas[3] R., Vartti[8] V.-P.
Affiliation(s)	1 Icelandic Radiation Safety Authority 2 Norwegian Radiation Protection Authority 3 University of Gothenburg, Sweden 4 University of the Faroe Islands 5 University of Iceland 6 Technical University of Denmark 7 Technical Research Centre of Finland 8 Radiation and Nuclear Safety Authority, Finland
ISBN	978-87-7893-407-9
Date	January 2015
Project	NKS-B / EFMARE
No. of pages	59
No. of tables	3
No. of illustrations	71
No. of references	20
Abstract max. 2000 characters	The goal of the EFMARE project is an analysis of consequences of radioactive releases into marine environment with special attention to the effects of the dynamic behaviour of the Nordic seas to radioecological assessments. The EFMARE project activity has planned to continue for two years (2014-2015). The main goals for 2014 is development and implementation of the bioaccumulation process into the models, improvement of the models, comparison with previous results and testing of the influence of the time of an accident for the radioecological consequences. Results of implementation of the kinetic model for bioaccumulation processes into the NRPA box model and the DETRA computer code clearly demonstrated that there is a significant quantitative difference between the kinetic modelling approach and the approach based on the constant concentration rates. Results of modelling were compared with experimental data on the basis of improved version of the NRPA box model for the Baltic Sea. It is clear demonstration that dynamic modelling of the bioaccumulation processes can provide a more correct description of the concentration of radionuclides in biota and, therefore, these results support the main goal of the EFMARE project. With a numerical case study the temporal variability of pollutant dispersal in Icelandic waters was demonstrated and discussed. The results emphasize the necessity to use operational hydrodynamic ocean models in order to forecast pollutant dispersal in Icelandic waters. The use of particle density can be used for comparison with simulations from the NRPA box model.
Key words	marine environment, hydrodynamic and box modelling, bioaccumulation submodel, accidents, radioecological consequences

Available on request from the NKS Secretariat, P.O.Box 49, DK-4000 Roskilde, Denmark.
Phone (+45) 4677 4041, e-mail nks@nks.org, www.nks.org